

International Telecommunication Union

**ITU-R**  
Radiocommunication Sector of ITU

**Recommendation ITU-R P.526-14**  
(01/2018)

**Propagation by diffraction**

**P Series**  
**Radiowave propagation**



## Foreword

The role of the Radiocommunication Sector is to ensure the rational, equitable, efficient and economical use of the radio-frequency spectrum by all radiocommunication services, including satellite services, and carry out studies without limit of frequency range on the basis of which Recommendations are adopted.

The regulatory and policy functions of the Radiocommunication Sector are performed by World and Regional Radiocommunication Conferences and Radiocommunication Assemblies supported by Study Groups.

## Policy on Intellectual Property Right (IPR)

ITU-R policy on IPR is described in the Common Patent Policy for ITU-T/ITU-R/ISO/IEC referenced in Annex 1 of Resolution ITU-R 1. Forms to be used for the submission of patent statements and licensing declarations by patent holders are available from <http://www.itu.int/ITU-R/go/patents/en> where the Guidelines for Implementation of the Common Patent Policy for ITU-T/ITU-R/ISO/IEC and the ITU-R patent information database can also be found.

### Series of ITU-R Recommendations

(Also available online at <http://www.itu.int/publ/R-REC/en>)

Series	Title
<b>BO</b>	Satellite delivery
<b>BR</b>	Recording for production, archival and play-out; film for television
<b>BS</b>	Broadcasting service (sound)
<b>BT</b>	Broadcasting service (television)
<b>F</b>	Fixed service
<b>M</b>	Mobile, radiodetermination, amateur and related satellite services
<b>P</b>	<b>Radiowave propagation</b>
<b>RA</b>	Radio astronomy
<b>RS</b>	Remote sensing systems
<b>S</b>	Fixed-satellite service
<b>SA</b>	Space applications and meteorology
<b>SF</b>	Frequency sharing and coordination between fixed-satellite and fixed service systems
<b>SM</b>	Spectrum management
<b>SNG</b>	Satellite news gathering
<b>TF</b>	Time signals and frequency standards emissions
<b>V</b>	Vocabulary and related subjects

*Note: This ITU-R Recommendation was approved in English under the procedure detailed in Resolution ITU-R 1.*

Electronic Publication  
Geneva, 2018

© ITU 2018

All rights reserved. No part of this publication may be reproduced, by any means whatsoever, without written permission of ITU.

## RECOMMENDATION ITU-R P.526-14

**Propagation by diffraction**

(Question ITU-R 202/3)

(1978-1982-1992-1994-1995-1997-1999-2001-2003-2005-2007-2009-2012-2013-2018)

**Scope**

This Recommendation presents several models to enable the reader to evaluate the effect of diffraction on the received field strength. The models are applicable to different obstacle types and to various path geometries.

The ITU Radiocommunication Assembly,

*considering*

that there is a need to provide engineering information for the calculation of field strengths over diffraction paths,

*recommends*

that the methods described in Annex 1 be used for the calculation of field strengths over diffraction paths, which may include a spherical earth surface, or irregular terrain with different kinds of obstacles.

**Annex 1****1 Introduction**

Although diffraction is produced only by the surface of the ground or other obstacles, account must be taken of the mean atmospheric refraction on the transmission path to evaluate the geometrical parameters situated in the vertical plane of the path (angle of diffraction, radius of curvature, height of obstacle). For this purpose, the path profile has to be traced with the appropriate equivalent Earth radius (Recommendation ITU-R P.834). If no other information is available, an equivalent Earth radius of 8 500 km may be taken as a basis.

**2 Basic concepts**

Diffraction of radiowaves over the Earth's surface is affected by terrain irregularities. In this context, before going further into the prediction methods for this propagation mechanism, a few basic concepts are given in this section.

## 2.1 Fresnel ellipsoids and Fresnel zones

In studying radiowave propagation between two points A and B, the intervening space can be subdivided by a family of ellipsoids, known as Fresnel ellipsoids, all having their focal points at A and B such that any point M on one ellipsoid satisfies the relation:

$$AM + MB = AB + n \frac{\lambda}{2} \quad (1)$$

where  $n$  is a whole number characterizing the ellipsoid and  $n = 1$  corresponds to the first Fresnel ellipsoid, etc., and  $\lambda$  is the wavelength.

As a practical rule, propagation is assumed to occur in line-of-sight (LoS), i.e. with negligible diffraction phenomena if there is no obstacle within the first Fresnel ellipsoid.

The radius of an ellipsoid at a point between the transmitter and the receiver can be approximated in self-consistent units by:

$$R_n = \left[ \frac{n \lambda d_1 d_2}{d_1 + d_2} \right]^{1/2} \quad (2)$$

or, in practical units:

$$R_n = 550 \left[ \frac{n d_1 d_2}{(d_1 + d_2) f} \right]^{1/2} \quad (3)$$

where  $f$  is the frequency (MHz) and  $d_1$  and  $d_2$  are the distances (km) between transmitter and receiver at the point where the ellipsoid radius (m) is calculated.

Some problems require consideration of Fresnel zones which are the zones obtained by taking the intersection of a family of ellipsoids by a plane. The zone of order  $n$  is the part between the curves obtained from ellipsoids  $n$  and  $n - 1$ , respectively.

## 2.2 Penumbra width

The transition from light to shadow defines the penumbra region. This transition takes place along a narrow strip (penumbra width) in the boundary of geometric shadow. Figure 1 shows the penumbra width ( $W$ ) in the case of a transmitter located a height,  $h$ , above a smooth spherical earth, which is given by:

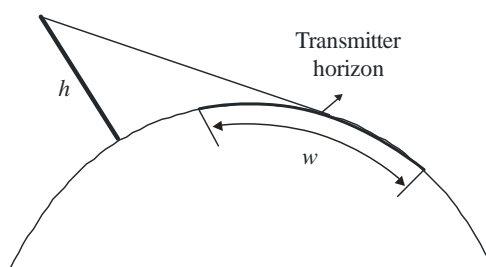
$$w = \left[ \frac{\lambda a_e^2}{\pi} \right]^{1/3} \text{ m} \quad (4)$$

where:

$\lambda$ : wavelength (m)

$a_e$ : effective Earth radius (m)

FIGURE 1  
Definition of penumbra width



P.0526-01

### 2.3 Diffraction zone

The diffraction zone of a transmitter extends from the LoS distance where the path clearance is equal to 60% of the first Fresnel zone radius, ( $R_1$ ), up to a distance well beyond the transmitter horizon where the mechanism of troposcatter becomes predominant.

### 2.4 Obstacle surface smoothness criterion

If the surface of the obstacle has irregularities not exceeding  $\Delta h$ ,  
where:

$$\Delta h = 0.04 [R\lambda^2]^{1/3} \quad \text{m} \quad (5)$$

where:

$R$ : obstacle curvature radius (m)

$\lambda$ : wavelength (m);

then the obstacle may be considered smooth and the methods described in §§ 3 and 4.2 may be used to calculate the attenuation.

### 2.5 Isolated obstacle

An obstacle can be considered isolated if there is no interaction between the obstacle itself and the surrounding terrain. In other words, the path attenuation is only due to the obstacle alone without any contribution from the remaining terrain. The following conditions must be satisfied:

- no overlapping between penumbra widths associated with each terminal and the obstacle top;
- the path clearance on both sides of the obstacles should be, at least, 0.6 of the first Fresnel zone radius;
- no specular reflection on both sides of the obstacle.

### 2.6 Types of terrain

Depending on the numerical value of the parameter  $\Delta h$  (see Recommendation ITU-R P.310) used to define the degree of terrain irregularities, three types of terrain can be classified:

#### a) *Smooth terrain*

The surface of the Earth can be considered smooth if terrain irregularities are of the order or less than  $0.1R$ , where  $R$  is the maximum value of the first Fresnel zone radius in the propagation path. In this case, the prediction model is based on the diffraction over the spherical Earth (see § 3).

#### b) *Isolated obstacles*

The terrain profile of the propagation path consists of one or more isolated obstacles. In this case, depending on the idealization used to characterize the obstacles encountered in the propagation path, the prediction models described in § 4 should be used.

c) *Rolling terrain*

The profile consists of several small hills, none of which form a dominant obstruction. Within its frequency range Recommendation ITU-R P.1546 is suitable for predicting field strength but it is not a diffraction method.

## 2.7 Fresnel integrals

The complex Fresnel integral is given by:

$$F_c(v) = \int_0^v \exp\left(j \frac{\pi s^2}{2}\right) ds = C(v) + jS(v) \quad (6)$$

where  $j$  is the complex operator equal to  $\sqrt{-1}$ , and  $C(v)$  and  $S(v)$  are the Fresnel cosine and sine integrals defined by:

$$C(v) = \int_0^v \cos\left(\frac{\pi s^2}{2}\right) ds \quad (7a)$$

$$S(v) = \int_0^v \sin\left(\frac{\pi s^2}{2}\right) ds \quad (7b)$$

The complex Fresnel integral  $F_c(v)$  can be evaluated by numerical integration, or with sufficient accuracy for most purposes for positive  $v$  using:

$$F_c(v) = \exp(jx) \sqrt{\frac{x}{4}} \sum_{n=0}^{11} \left[ (a_n - jb_n) \left(\frac{x}{4}\right)^n \right] \quad \text{for } 0 \leq x < 4 \quad (8a)$$

$$F_c(v) = \left(\frac{1+j}{2}\right) + \exp(jx) \sqrt{\frac{4}{x}} \sum_{n=0}^{11} \left[ (c_n - jd_n) \left(\frac{4}{x}\right)^n \right] \quad \text{for } x \geq 4 \quad (8b)$$

where:

$$x = 0.5\pi v^2 \quad (9)$$

and  $a_n$ ,  $b_n$ ,  $c_n$  and  $d_n$  are the Boersma coefficients given below:

$a_0 = +1.595769140$	$b_0 = -0.000000033$	$c_0 = +0.000000000$	$d_0 = +0.199471140$
$a_1 = -0.000001702$	$b_1 = +4.255387524$	$c_1 = -0.024933975$	$d_1 = +0.000000023$
$a_2 = -6.808568854$	$b_2 = -0.000092810$	$c_2 = +0.000003936$	$d_2 = -0.009351341$
$a_3 = -0.000576361$	$b_3 = -7.780020400$	$c_3 = +0.005770956$	$d_3 = +0.000023006$
$a_4 = +6.920691902$	$b_4 = -0.009520895$	$c_4 = +0.000689892$	$d_4 = +0.004851466$
$a_5 = -0.016898657$	$b_5 = +5.075161298$	$c_5 = -0.009497136$	$d_5 = +0.001903218$
$a_6 = -3.050485660$	$b_6 = -0.138341947$	$c_6 = +0.011948809$	$d_6 = -0.017122914$
$a_7 = -0.075752419$	$b_7 = -1.363729124$	$c_7 = -0.006748873$	$d_7 = +0.029064067$
$a_8 = +0.850663781$	$b_8 = -0.403349276$	$c_8 = +0.000246420$	$d_8 = -0.027928955$
$a_9 = -0.025639041$	$b_9 = +0.702222016$	$c_9 = +0.002102967$	$d_9 = +0.016497308$
$a_{10} = -0.150230960$	$b_{10} = -0.216195929$	$c_{10} = -0.001217930$	$d_{10} = -0.005598515$
$a_{11} = +0.034404779$	$b_{11} = +0.019547031$	$c_{11} = +0.000233939$	$d_{11} = +0.000838386$

$C(v)$  and  $S(v)$  may be evaluated for negative values of  $v$  by noting that:

$$C(-v) = -C(v) \quad (10a)$$

$$S(-v) = -S(v) \quad (10b)$$

### 3 Diffraction over a spherical Earth

The additional transmission loss due to diffraction over a spherical Earth can be computed by the classical residue series formula. A computer program GRWAVE, available from the ITU, provides the complete method. A subset of the outputs from this program (for antennas close to the ground and at lower frequencies) is presented in Recommendation ITU-R P.368.

The following subsections describe numerical and nomogram methods which may be used for frequencies 10 MHz and above. For frequencies below 10 MHz, GRWAVE should always be used. Section 3.1 gives methods for over-the-horizon paths. Section 3.1.1 is a numerical method. Section 3.1.2 is a nomogram method. Section 3.2 is a method applicable for the smooth earth case for any distance and for frequencies 10 MHz and above. This utilizes the numerical method in § 3.1.1.

#### 3.1 Diffraction loss for over-the-horizon paths

At long distances over the horizon, only the first term of the residue series is important. Even near or at the horizon this approximation can be used with a maximum error around 2 dB in most cases.

This first term can be written as the product of a distance term,  $F$ , and two height gain terms,  $G_T$  and  $G_R$ . Sections 3.1.1 and 3.1.2 describe how these terms can be obtained from simple formula or from nomograms.

##### 3.1.1 Numerical calculation

###### 3.1.1.1 Influence of the electrical characteristics of the surface of the Earth

The extent to which the electrical characteristics of the surface of the Earth influence the diffraction loss can be determined by calculating a normalized factor for surface admittance,  $K$ , given by the formulae:

in self-consistent units:

$$K_H = \left( \frac{2\pi a_e}{\lambda} \right)^{-1/3} \left[ (\varepsilon - 1)^2 + (60 \lambda \sigma)^2 \right]^{-1/4} \quad \text{for horizontal polarization} \quad (11)$$

and

$$K_V = K_H \left[ \varepsilon^2 + (60 \lambda \sigma)^2 \right]^{1/2} \quad \text{for vertical polarization} \quad (12)$$

or, in practical units:

$$K_H = 0.36 (a_e f)^{-1/3} \left[ (\varepsilon - 1)^2 + (18\,000 \sigma / f)^2 \right]^{-1/4} \quad (11a)$$

$$K_V = K_H \left[ \varepsilon^2 + (18\,000 \sigma / f)^2 \right]^{1/2} \quad (12a)$$

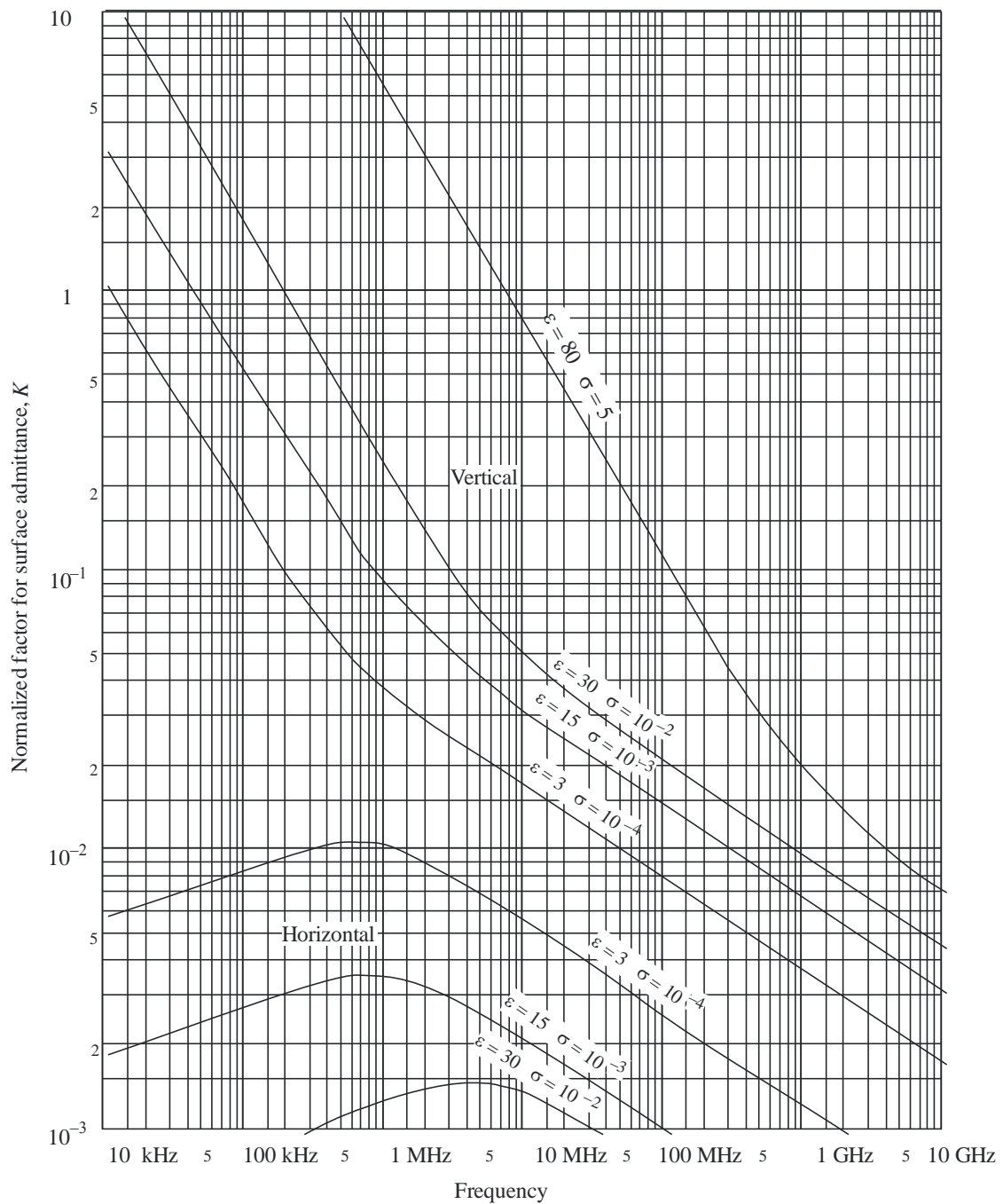
where:

$a_e$ : effective radius of the Earth (km)

- $\epsilon$ : effective relative permittivity  
 $\sigma$ : effective conductivity (S/m)  
 $f$ : frequency (MHz).

Typical values of  $K$  are shown in Fig. 2.

FIGURE 2  
Calculation of  $K$



If  $K$  is less than 0.001, the electrical characteristics of the Earth are not important. For values of  $K$  greater than 0.001 and less than 1, the appropriate formulae given in § 3.1.1.2 can be used. When  $K$  has a value greater than about 1, the diffraction field strength calculated using the method of § 3.1.1.2



differs from the results given by the computer program GRWAVE, and the difference increases rapidly as  $K$  increases. GRWAVE should be used for  $K$  greater than 1. This only occurs for vertical polarization, at frequencies below 10 MHz over sea, or below 200 kHz over land. In all other cases the method of § 3.1.1.2 is valid.

### 3.1.1.2 Diffraction field strength formulae

The diffraction field strength,  $E$ , relative to the free-space field strength,  $E_0$ , is given by the formula:

$$20 \log \frac{E}{E_0} = F(X) + G(Y_1) + G(Y_2) \quad \text{dB} \quad (13)$$

where  $X$  is the normalized length of the path between the antennas at normalized heights  $Y_1$  and  $Y_2$  (and where  $20 \log \frac{E}{E_0}$  is generally negative).

In self-consistent units:

$$X = \beta \left( \frac{\pi}{\lambda a_e^2} \right)^{1/3} d \quad (14)$$

$$Y = 2\beta \left( \frac{\pi^2}{\lambda^2 a_e} \right)^{1/3} h \quad (15)$$

or, in practical units:

$$X = 2.188 \beta f^{1/3} a_e^{-2/3} d \quad (14a)$$

$$Y = 9.575 \times 10^{-3} \beta f^{2/3} a_e^{-1/3} h \quad (15a)$$

where:

- $d$ : path length (km)
- $a_e$ : equivalent Earth's radius (km)
- $h$ : antenna height (m)
- $f$ : frequency (MHz).

$\beta$  is a parameter allowing for the type of ground and for polarization. It is related to  $K$  by the following semi-empirical formula:

$$\beta = \frac{1 + 1.6 K^2 + 0.67 K^4}{1 + 4.5 K^2 + 1.53 K^4} \quad (16)$$

For horizontal polarization at all frequencies, and for vertical polarization above 20 MHz over land or 300 MHz over sea,  $\beta$  may be taken as equal to 1.

For vertical polarization below 20 MHz over land or 300 MHz over sea,  $\beta$  must be calculated as a function of  $K$ . However, it is then possible to disregard  $\epsilon$  and write:

$$K^2 \approx 6.89 \frac{\sigma}{k^{2/3} f^{5/3}} \quad (16a)$$

where  $\sigma$  is expressed in S/m,  $f$  (MHz) and  $k$  is the multiplying factor of the Earth's radius.

The distance term is given by the formula:

$$F(X) = 11 + 10 \log(X) - 17.6 X \quad \text{for } X \geq 1.6 \quad (17a)$$

$$F(X) = -20 \log(X) - 5.6488X^{1.425} \quad \text{for } X < 1.6 \quad (17b)$$

The height gain term,  $G(Y)$  is given by the following formulae:

$$G(Y) \cong 17.6(B-1.1)^{1/2} - 5 \log(B-1.1) - 8 \quad \text{for } B > 2 \quad (18)$$

$$G(Y) \cong 20 \log(B+0.1B^3) \quad \text{for } B \leq 2 \quad (18a)$$

If  $G(Y) < 2 + 20 \log K$ , set  $G(Y)$  to the value  $2 + 20 \log K$

In the above:

$$B = \beta Y \quad (18b)$$

The accuracy of the diffracted field strength given by equation (13) is limited by the approximation inherent in only using the first term of the residue series. Equation (13) is accurate to better than 2 dB for values of  $X$ ,  $Y_1$  and  $Y_2$  that are constrained by the formula:

$$X - (\beta Y_1)^{1/2} \Delta(Y_1, K) - (\beta Y_2)^{1/2} \Delta(Y_2, K) > X_{lim} \quad (19)$$

where:

$$X_{lim} = 1.096 - 1.280(1 - \beta) \quad (19a)$$

$$\Delta(Y, K) = \Delta(Y, 0) + 1.779(1 - \beta)[\Delta(Y, \infty) - \Delta(Y, 0)] \quad (19b)$$

$\Delta(Y, 0)$  and  $\Delta(Y, \infty)$  are given by:

$$\Delta(Y, 0) = 0.5 \left[ 1 + \tanh \left( \frac{0.5 \log(\beta Y) - 0.255}{0.3} \right) \right] \quad (19c)$$

$$\Delta(Y, \infty) = 0.5 \left[ 1 + \tanh \left( \frac{0.5 \log(\beta Y) + 0.255}{0.25} \right) \right] \quad (19d)$$

Consequently, the minimum distance  $d_{min}$  for which equation (13) is valid is given by:

$$X_{min} = X_{lim} + (\beta Y_1)^{1/2} \Delta(Y_1, K) + (\beta Y_2)^{1/2} \Delta(Y_2, K) \quad (19e)$$

and  $d_{min}$  is obtained from  $X_{min}$  using equation (14a).

### 3.1.2 Calculation by nomograms

Under the same approximation condition (the first term of the residue series is dominant), the calculation may also be made using the following formula:

$$20 \log \frac{E}{E_0} = F(d) + H(h_1) + H(h_2) \quad \text{dB} \quad (20)$$

where:

$E$ : received field strength

$E_0$ : field strength in free space at the same distance

$d$ : distance between the extremities of the path

$h_1$  and  $h_2$ : heights of the antennas above the spherical earth.

The function  $F$  (influence of the distance) and  $H$  (height-gain) are given by the nomograms in Figs 3, 4, 5 and 6.

These nomograms (Figs 3 to 6) give directly the received level relative to free space, for  $k = 1$  and  $k = 4/3$ , and for frequencies greater than approximately 30 MHz.  $k$  is the effective Earth radius factor, defined in Recommendation ITU-R P.310. However, the received level for other values of  $k$  may be calculated by using the frequency scale for  $k = 1$ , but replacing the frequency in question by a hypothetical frequency equal to  $f/k^2$  for Figs 3 and 5, and  $f/\sqrt{k}$  for Figs 4 and 6.

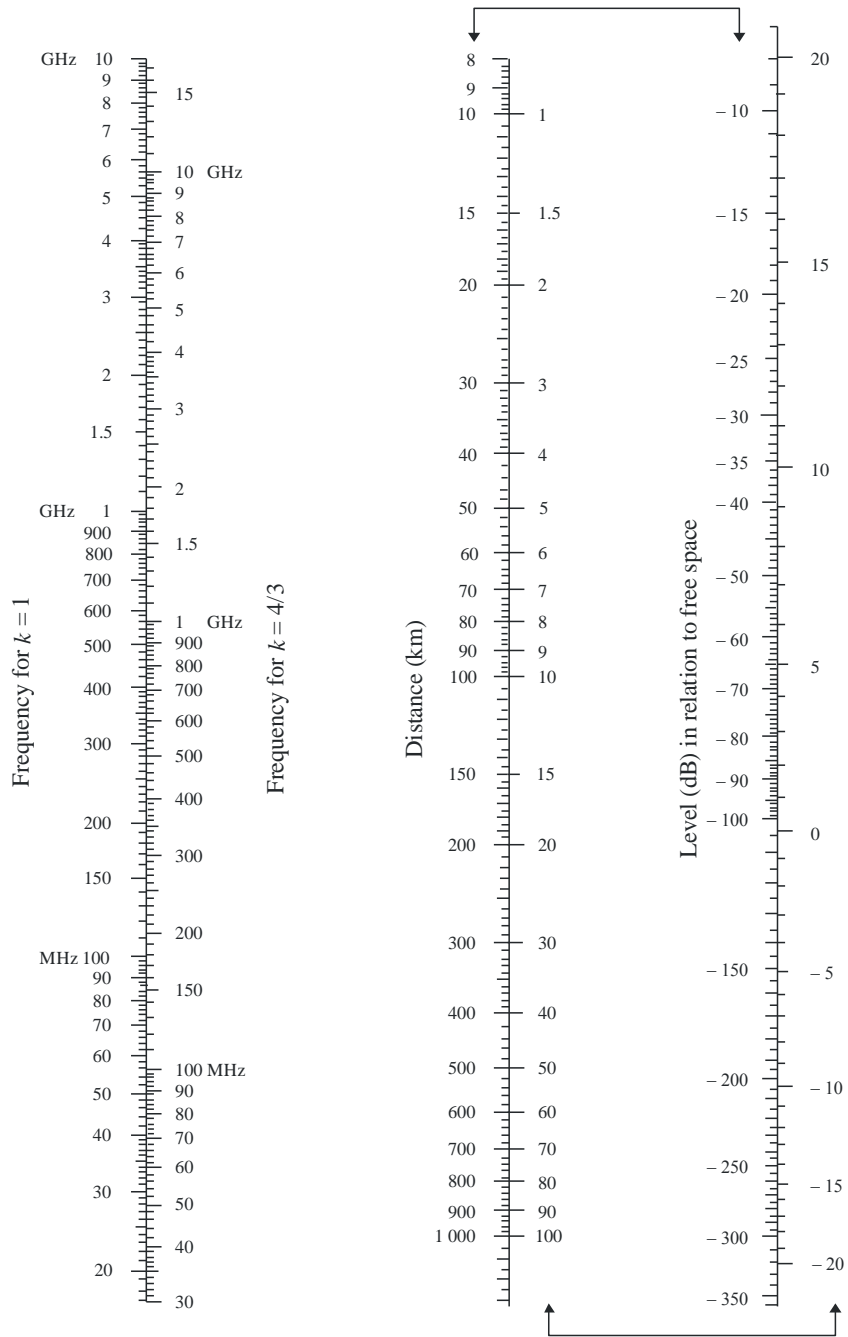
Very close to the ground the field strength is practically independent of the height. This phenomenon is particularly important for vertical polarization over the sea. For this reason Fig. 6 includes a heavy black vertical line AB. If the straight line should intersect this heavy line AB, the real height should be replaced by a larger value, so that the straight line just touches the top of the limit line at A.

NOTE 1 – Attenuation relative to free space is given by the negative of the values given by equation (20). If equation (20) gives a value above the free-space field, the method is invalid.

NOTE 2 – The effect of line AB is included in the numerical method given in § 3.1.1.

FIGURE 3

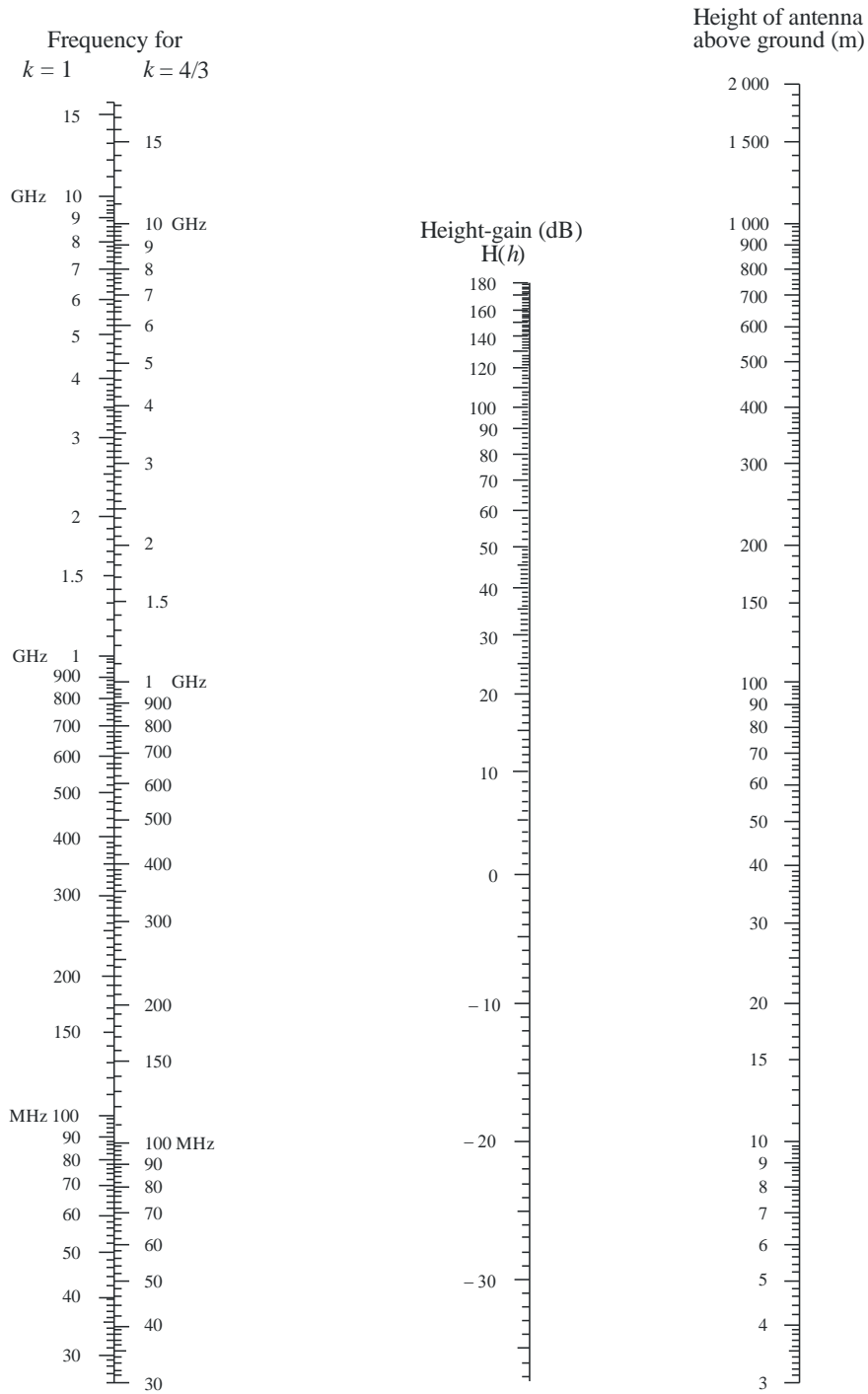
Diffraction by a spherical Earth – effect of distance



Horizontal polarization over land and sea  
 Vertical polarization over land

(The scales joined by arrows should be used together)

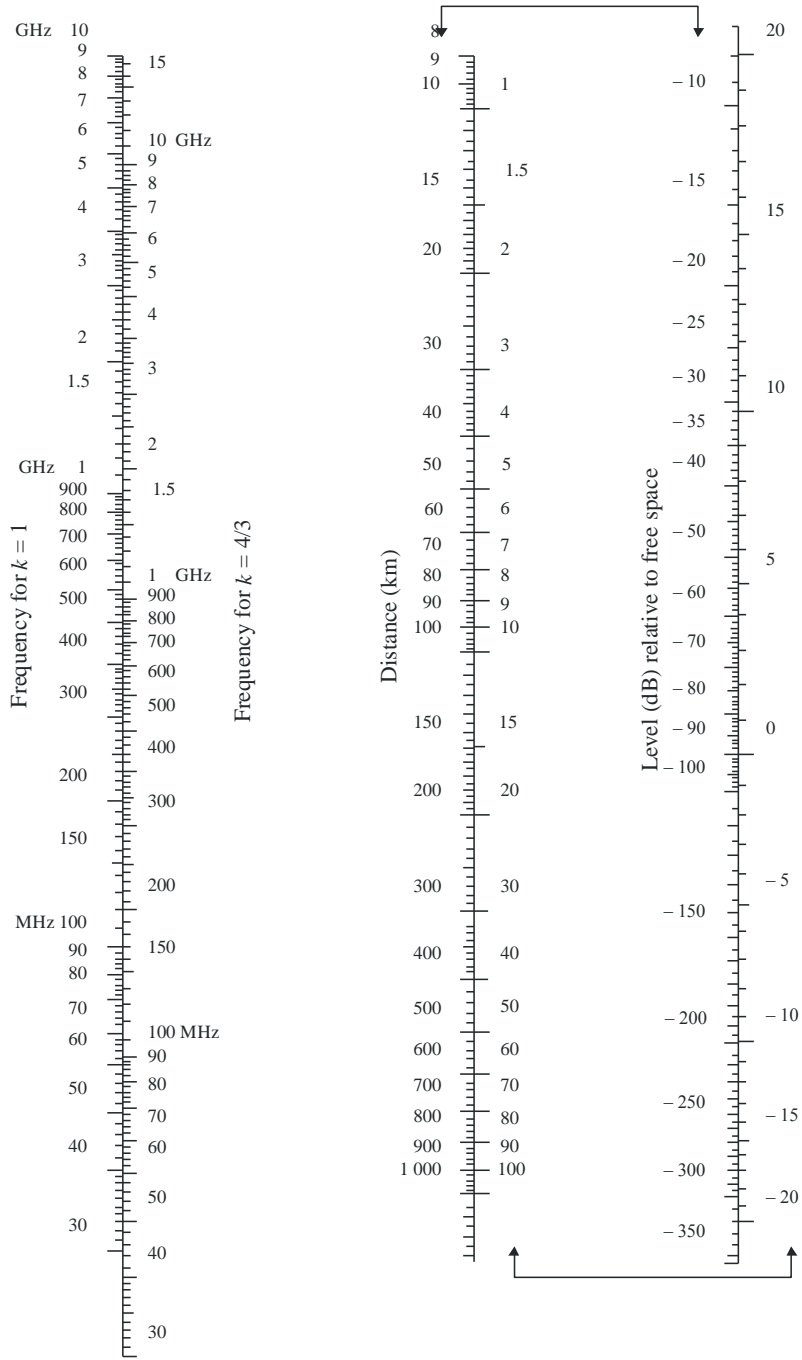
FIGURE 4  
 Diffraction by a spherical Earth – height-gain



Horizontal polarization – land and sea  
 Vertical polarization – land

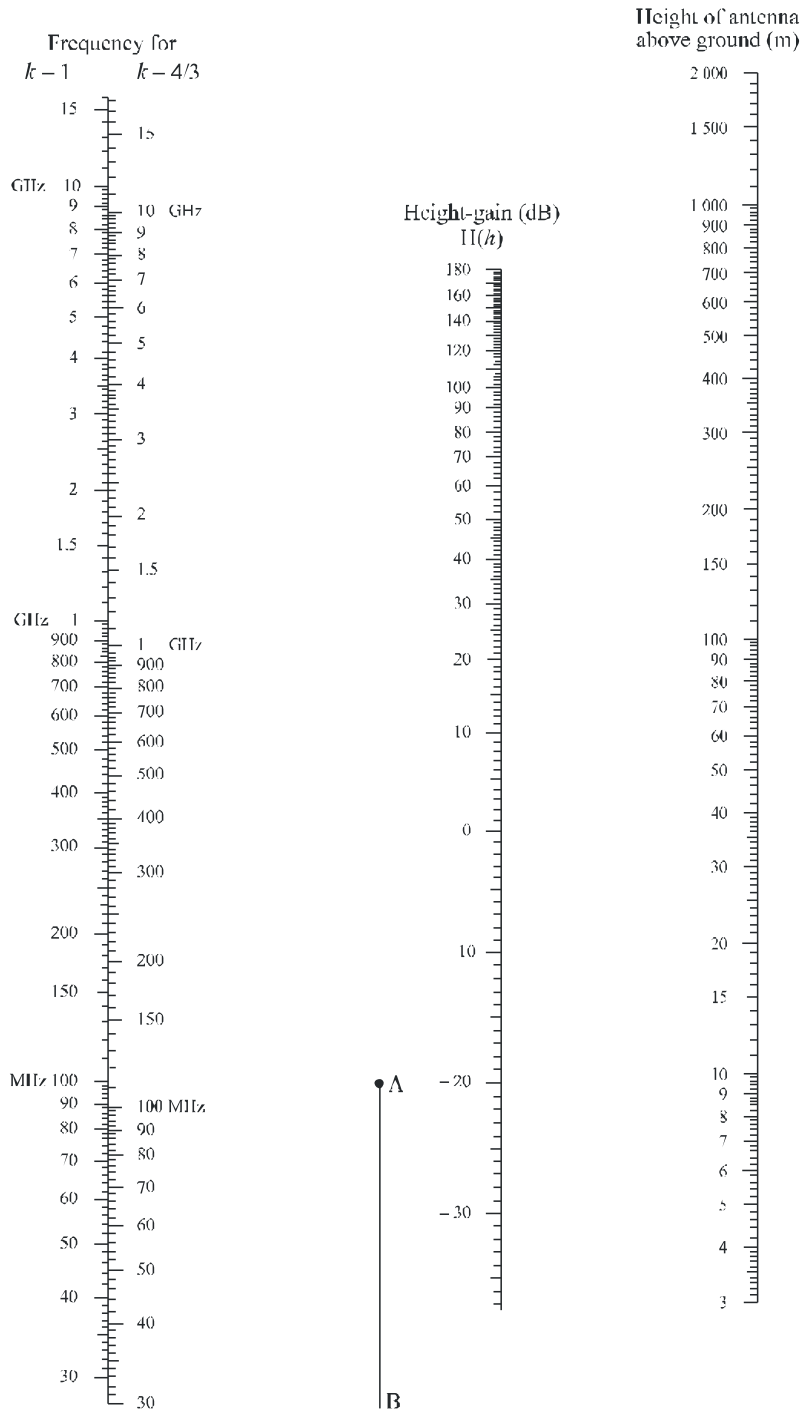
FIGURE 5

Diffraction by a spherical Earth – effect of distance



Vertical polarization over sea  
 (The scales joined by arrows should be used together)

FIGURE 6  
 Diffraction by a spherical Earth – height-gain



Vertical polarization – sea

### 3.2 Diffraction loss for any distance at 10 MHz and above

The following step-by-step procedure should be used for a spherical-earth path of any length at frequencies of 10 MHz and above, for effective Earth radius  $a_e > 0$ . The method uses the calculation in § 3.1.1 for over-the-horizon cases, and otherwise an interpolation procedure based on a notional effective-earth radius.

The procedure uses self-consistent units and proceeds as follows:

Calculate the marginal LoS distance given by:

$$d_{los} = \sqrt{2a_e} (\sqrt{h_1} + \sqrt{h_2}) \quad (21)$$

If  $d \geq d_{los}$  calculate diffraction loss using the method in § 3.1.1. No further calculation is necessary.

Otherwise continue:

Calculate the smallest clearance height between the curved-earth path and the ray between the antennas,  $h$  (see Fig. 7), given by:

$$h = \frac{\left(h_1 - \frac{d_1^2}{2a_e}\right)d_2 + \left(h_2 - \frac{d_2^2}{2a_e}\right)d_1}{d} \quad (22)$$

$$d_1 = \frac{d}{2} (1 + b) \quad (22a)$$

$$d_2 = d - d_1 \quad (22b)$$

$$b = 2\sqrt{\frac{m+1}{3m}} \cos \left\{ \frac{\pi}{3} + \frac{1}{3} \arccos \left( \frac{3c}{2} \sqrt{\frac{3m}{(m+1)^3}} \right) \right\} \quad (22c)$$

$$c = \frac{h_1 - h_2}{h_1 + h_2} \quad (22d)$$

$$m = \frac{d^2}{4a_e(h_1 + h_2)} \quad (22e)$$

Calculate the required clearance for zero diffraction loss,  $h_{req}$ , given by:

$$h_{req} = 0.552 \sqrt{\frac{d_1 d_2 \lambda}{d}} \quad (23)$$

If  $h > h_{req}$  the diffraction loss for the path is zero. No further calculation is required.

Otherwise continue:

Calculate the modified effective earth radius,  $a_{em}$ , which gives marginal LoS at distance  $d$  given by:



$$a_{em} = 0.5 \left( \frac{d}{\sqrt{h_1} + \sqrt{h_2}} \right)^2 \tag{24}$$

Use the method in § 3.1.1 to calculate the diffraction loss for the path using the modified effective earth radius  $a_{em}$  in place of the effective earth radius  $a_e$ , and designate this loss  $A_h$ .

If  $A_h$  is negative, the diffraction loss for the path is zero, and no further calculation is necessary.

Otherwise calculate the interpolated diffraction loss,  $A$  (dB), given by:

$$A = \left[ 1 - h/h_{req} \right] A_h \tag{25}$$

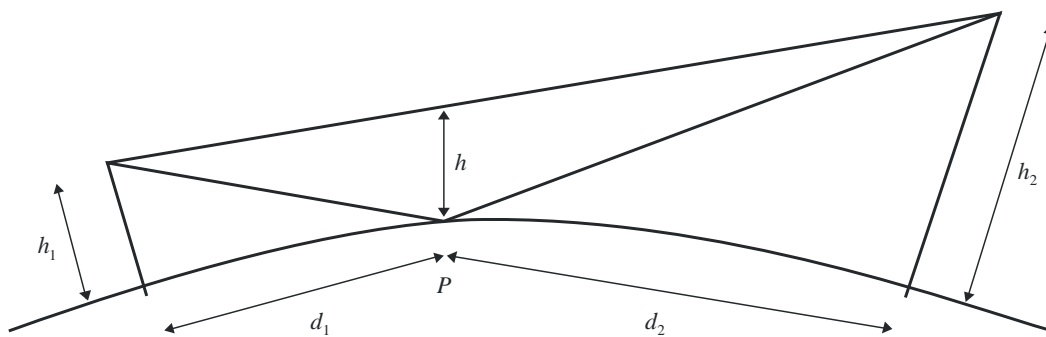
#### 4 Diffraction over isolated obstacles or a general terrestrial path

Many propagation paths encounter one obstacle or several separate obstacles and it is useful to estimate the losses caused by such obstacles. To make such calculations, it is necessary to idealize the form of the obstacles, either assuming a knife-edge of negligible thickness or a thick smooth obstacle with a well-defined radius of curvature at the top. Real obstacles have, of course, more complex forms, so that the indications provided in this Recommendation should be regarded only as an approximation. These models do not take into account the profile transverse to the direction of the radio link, which may have a significant effect on diffraction loss.

In those cases where the direct path between the terminals is much shorter than the diffraction path, it is necessary to calculate the additional transmission loss due to the longer path.

The data given below apply when the wavelength is fairly small in relation to the size of the obstacles, i.e. mainly to VHF and shorter waves ( $f > 30$  MHz).

FIGURE 7  
Path clearance



P: Reflection point

P.0526-07

##### 4.1 Single knife-edge obstacle

In this extremely idealized case (see Figs 8a) and 8b)), all the geometrical parameters are combined together in a single dimensionless parameter normally denoted by  $v$  which may assume a variety of equivalent forms according to the geometrical parameters selected:

$$v = h \sqrt{\frac{2}{\lambda} \left( \frac{1}{d_1} + \frac{1}{d_2} \right)} \quad (26)$$

$$v = \theta \sqrt{\frac{2}{\lambda \left( \frac{1}{d_1} + \frac{1}{d_2} \right)}} \quad (27)$$

$$v = \sqrt{\frac{2 h \theta}{\lambda}} \quad (v \text{ has the sign of } h \text{ and } \theta) \quad (28)$$

$$v = \sqrt{\frac{2 d}{\lambda} \cdot \alpha_1 \alpha_2} \quad (v \text{ has the sign of } \alpha_1 \text{ and } \alpha_2) \quad (29)$$

where:

- $h$ : height of the top of the obstacle above the straight line joining the two ends of the path. If the height is below this line,  $h$  is negative
- $d_1$  and  $d_2$ : distances of the two ends of the path from the top of the obstacle
- $d$ : length of the path
- $\theta$ : angle of diffraction (rad); its sign is the same as that of  $h$ . The angle  $\theta$  is assumed to be less than about 0.2 rad, or roughly 12°
- $\alpha_1$  and  $\alpha_2$ : angles in radians between the top of the obstacle and one end as seen from the other end.  $\alpha_1$  and  $\alpha_2$  are of the sign of  $h$  in the above equations.

NOTE 1 – In equations (26) to (29) inclusive  $h$ ,  $d$ ,  $d_1$ ,  $d_2$  and  $\lambda$  should be in self-consistent units.

FIGURE 8

Geometrical elements

(For definitions of  $\theta$ ,  $\alpha_1$ ,  $\alpha_2$ ,  $d$ ,  $d_1$ ,  $d_2$  and  $R$ , see § 4.1 and 4.2)

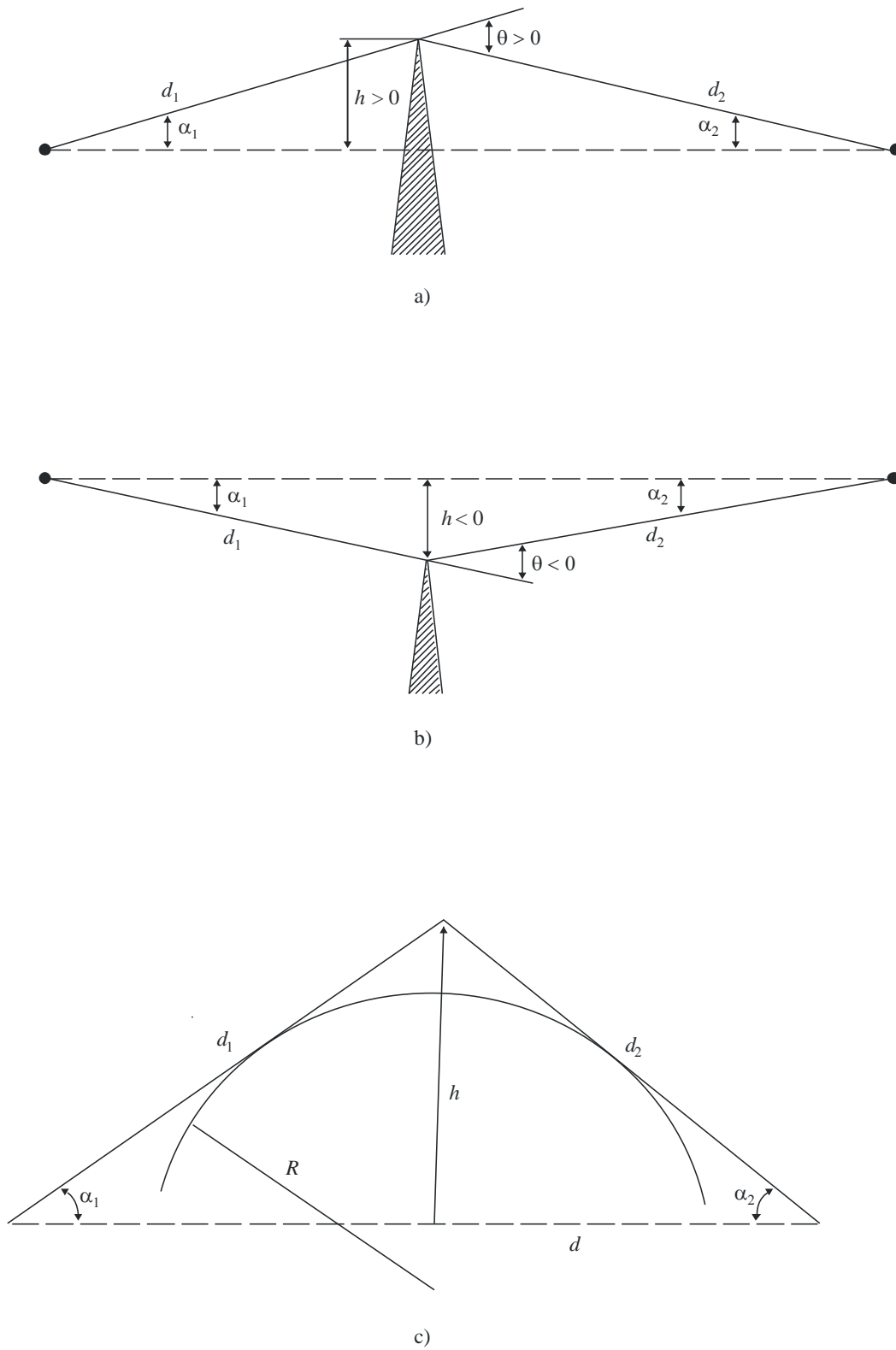


Figure 9 gives, as a function of  $v$ , the loss  $J(v)$  (dB).

$J(v)$  is given by:

$$J(v) = -20 \log \left( \frac{\sqrt{[1 - C(v) - S(v)]^2 + [C(v) - S(v)]^2}}{2} \right) \quad (30)$$

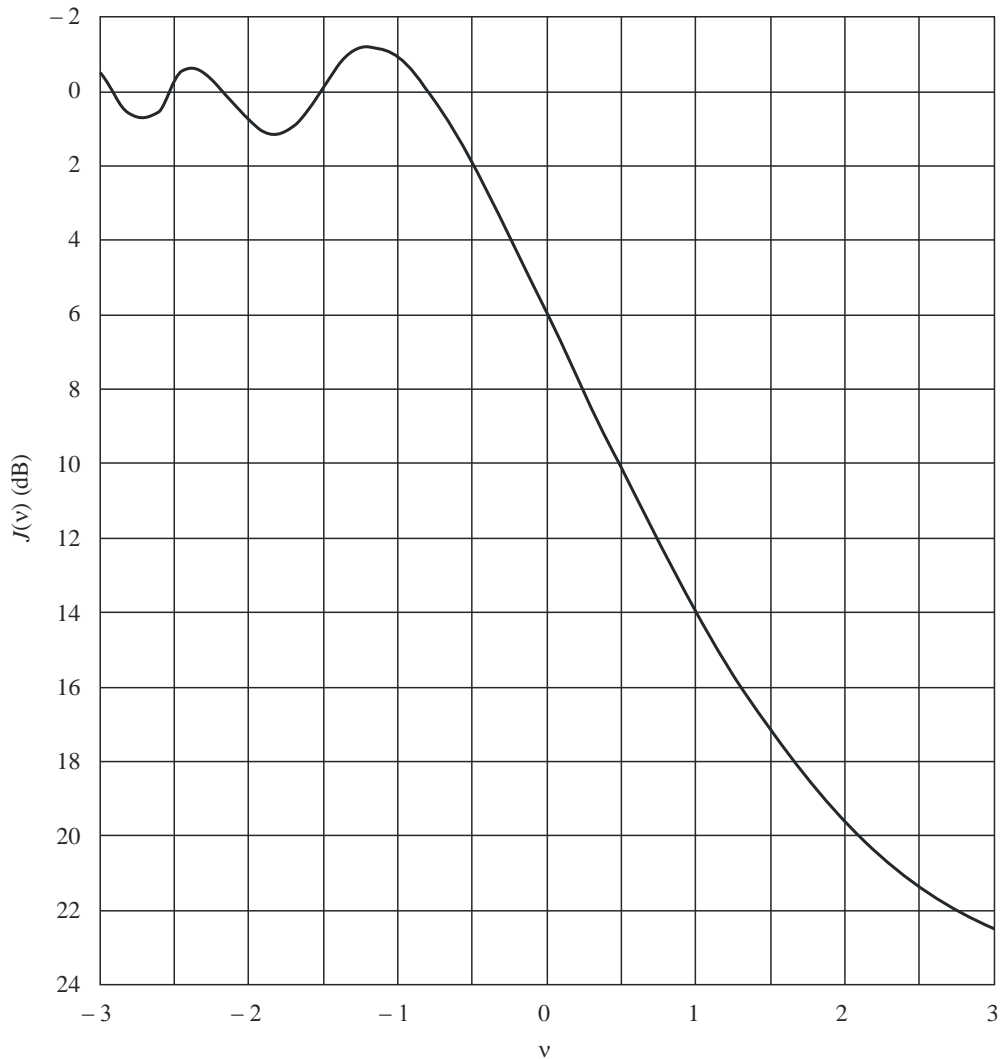
where  $C(v)$  and  $S(v)$  are the real and imaginary parts respectively of the complex Fresnel integral  $F(v)$  defined in § 2.7.

For  $v$  greater than  $-0.78$  an approximate value can be obtained from the expression:

$$J(v) = 6.9 + 20 \log \left( \sqrt{(v - 0.1)^2 + 1} + v - 0.1 \right) \quad \text{dB} \quad (31)$$

FIGURE 9

Knife-edge diffraction loss



### 4.2 Single rounded obstacle

The geometry of a rounded obstacle of radius  $R$  is illustrated in Fig. 8c). Note that the distances  $d_1$  and  $d_2$ , and the height  $h$  above the baseline, are all measured to the vertex where the projected rays intersect above the obstacle. The diffraction loss for this geometry may be calculated as:

$$A = J(v) + T(m,n) \quad \text{dB} \quad (32)$$

where:

- a)  $J(v)$  is the Fresnel-Kirchoff loss due to an equivalent knife-edge placed with its peak at the vertex point. The dimensionless parameter  $v$  may be evaluated from any of equations (26) to (29) inclusive. For example, in practical units equation (26) may be written:

$$v = 0.0316 h \left[ \frac{2(d_1 + d_2)}{\lambda d_1 d_2} \right]^{1/2} \quad (33)$$

where  $h$  and  $\lambda$  are in metres, and  $d_1$  and  $d_2$  are in kilometres.

$J(v)$  may be obtained from Fig. 9 or from equation (31). Note that for an obstruction to LoS propagation,  $v$  is positive and equation (31) is valid.

- b)  $T(m,n)$  is the additional attenuation due to the curvature of the obstacle:

$$T(m,n) = 7.2m^{1/2} - (2 - 12.5n)m + 3.6m^{3/2} - 0.8m^2 \text{ dB} \quad \text{for } mn \leq 4 \quad (34a)$$

$$T(m,n) = -6 - 20 \log(mn) + 7.2m^{1/2} - (2 - 17n)m + 3.6m^{3/2} - 0.8m^2 \text{ dB} \quad \text{for } mn > 4 \quad (34b)$$

and

$$m = R \left[ \frac{d_1 + d_2}{d_1 d_2} \right] \left/ \left[ \frac{\pi R}{\lambda} \right]^{1/3} \right. \quad (35)$$

$$n = h \left[ \frac{\pi R}{\lambda} \right]^{2/3} \left/ R \right. \quad (36)$$

and  $R, d_1, d_2, h$  and  $\lambda$  are in self-consistent units.

Note that as  $R$  tends to zero,  $T(m,n)$  also tend to zero. Thus equation (32) reduces to knife-edge diffraction for a cylinder of zero radius.

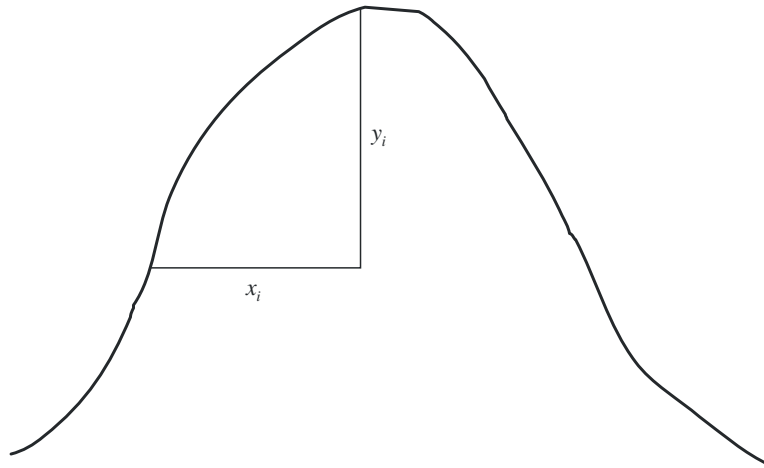
The obstacle radius of curvature corresponds to the radius of curvature at the apex of a parabola fitted to the obstacle profile in the vicinity of the top. When fitting the parabola, the maximum vertical distance from the apex to be used in this procedure should be of the order of the first Fresnel zone radius where the obstacle is located. An example of this procedure is shown in Fig. 10, where:

$$y_i = \frac{x_i^2}{2r_i} \quad (37)$$

and  $r_i$  is the radius of curvature corresponding to the sample  $i$  of the vertical profile of the ridge. In the case of  $N$  samples, the median radius of curvature of the obstacle is given by:

$$r = \frac{1}{N} \sum_1^N \frac{x_i^2}{2y_i} \quad (38)$$

FIGURE 10  
Vertical profile of the obstacle



P.0526-10

### 4.3 Double isolated edges

This method consists of applying single knife-edge diffraction theory successively to the two obstacles, with the top of the first obstacle acting as a source for diffraction over the second obstacle (see Fig. 11). The first diffraction path, defined by the distances  $a$  and  $b$  and the height  $h'_1$ , gives a loss  $L_1$  (dB). The second diffraction path, defined by the distances  $b$  and  $c$  and the height  $h'_2$ , gives a loss  $L_2$  (dB).  $L_1$  and  $L_2$  are calculated using formulae of § 4.1. A correction term  $L_c$  (dB) must be added to take into account the separation  $b$  between the edges.  $L_c$  may be estimated by the following formula:

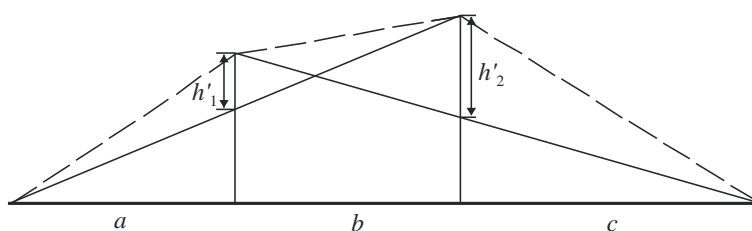
$$L_c = 10 \log \left[ \frac{(a + b)(b + c)}{b(a + b + c)} \right] \quad (39)$$

which is valid when each of  $L_1$  and  $L_2$  exceeds about 15 dB. The total diffraction loss is then given by:

$$L = L_1 + L_2 + L_c \quad (40)$$

The above method is particularly useful when the two edges give similar losses.

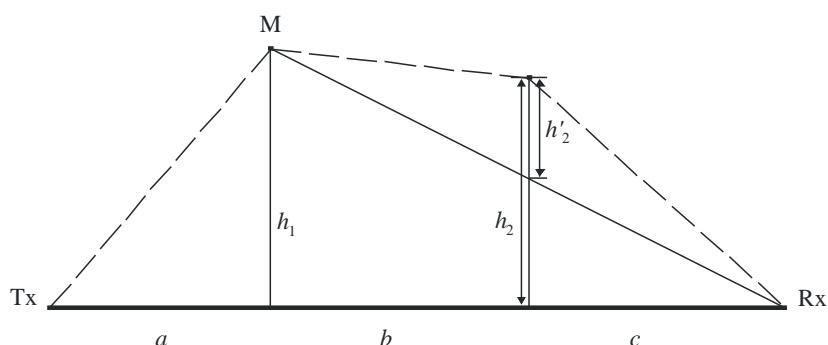
FIGURE 11  
Method for double isolated edges



P.0526-11

If one edge is predominant (see Fig. 12), the first diffraction path is defined by the distances  $a$  and  $b + c$  and the height  $h_1$ . The second diffraction path is defined by the distances  $b$  and  $c$  and the height  $h'_2$ .

FIGURE 12  
Figure showing the main and the second obstacle



P.0526-12

The method consists of applying single knife-edge diffraction theory successively to the two obstacles. First, the higher  $h/r$  ratio determines the main obstacle, M, where  $h$  is the edge height from the direct path TxRx as shown in Fig. 12, and  $r$  is the first Fresnel ellipsoid radius given by equation (2). Then  $h'_2$ , the height of the secondary obstacle from the sub-path MR, is used to calculate the loss caused by this secondary obstacle. A correction term  $T_c$  (dB) must be subtracted, in order to take into account the separation between the two edges as well as their height.  $T_c$  (dB) may be estimated by the following formula:

$$T_c = \left[ 12 - 20 \log_{10} \left( \frac{2}{1 - \frac{\alpha}{\pi}} \right) \right] \left( \frac{q}{p} \right)^{2p} \quad (41)$$

with:

$$p = \left[ \frac{2}{\lambda} \frac{(a + b + c)}{(b + c)a} \right]^{1/2} h_1 \quad (42a)$$

$$q = \left[ \frac{2}{\lambda} \frac{(a + b + c)}{(a + b)c} \right]^{1/2} h_2 \quad (42b)$$

$$\tan \alpha = \left[ \frac{b(a+b+c)}{ac} \right]^{1/2} \quad (42c)$$

$h_1$  and  $h_2$  are the edge heights from the direct path transmitter-receiver.

The total diffraction loss is given by:

$$L = L_1 + L_2 - T_c \quad (43)$$

The same method may be applied to the case of rounded obstacles using § 4.3.

In cases where the diffracting obstacle may be clearly identified as a flat-roofed building a single knife-edge approximation is not sufficient. It is necessary to calculate the phasor sum of two components: one undergoing a double knife-edge diffraction and the other subject to an additional reflection from the roof surface. It has been shown that, where the reflectivity of the roof surface and any difference in height between the roof surface and the side walls are not accurately known, then a double knife-edge model produces a good prediction of the diffracted field strength, ignoring the reflected component.

#### 4.4 Multiple isolated cylinders

This method is recommended for diffraction over irregular terrain which forms one or more obstacles to LoS propagation where each obstacle can be represented by a cylinder with a radius equal to the radius of curvature at the obstacle top, being advisable when detailed vertical profile through the ridge is available.

The terrain height profile should be available as a set of samples of ground height above sea level, the first and last being the heights of the transmitter and receiver above sea level. Atmospheric refractivity gradient should be taken into account via the concept of effective Earth radius. Distance and height values are described as though stored in arrays indexed from 1 to  $N$ , where  $N$  equals the number of profile samples.

In the following a systematic use of suffices is made:

- $h_i$ : height above sea level of the  $i$ -th point
- $d_i$ : distance from the transmitter to the  $i$ -th point
- $d_{ij}$ : distance from the  $i$ -th to the  $j$ -th points.

The first step is to perform a “stretched string” analysis of the profile. This identifies the sample points which would be touched by a string stretched over the profile from transmitter to receiver. This may be done by the following procedure, in which all values of height and distance are in self-consistent units, and all angles are in radians. The method includes approximations which are valid for radio paths making small angles to the horizontal. If a path has ray gradients exceeding about  $5^\circ$  more exact geometry may be justified.

Each string point is identified as the profile point with the highest angular elevation above the local horizontal as viewed from the previous string point, starting at one end of the profile and finishing at the other. Viewed from point  $s$ , the elevation of the  $i$ -th profile sample ( $i > s$ ) is given by:

$$e = [(h_i - h_s) / d_{si}] - [d_{si} / 2a_e] \quad (44)$$

where:



$$\begin{aligned} a_e: & \text{ effective Earth radius, given by:} \\ & = k \times 6371 \text{ (km)} \end{aligned}$$

and

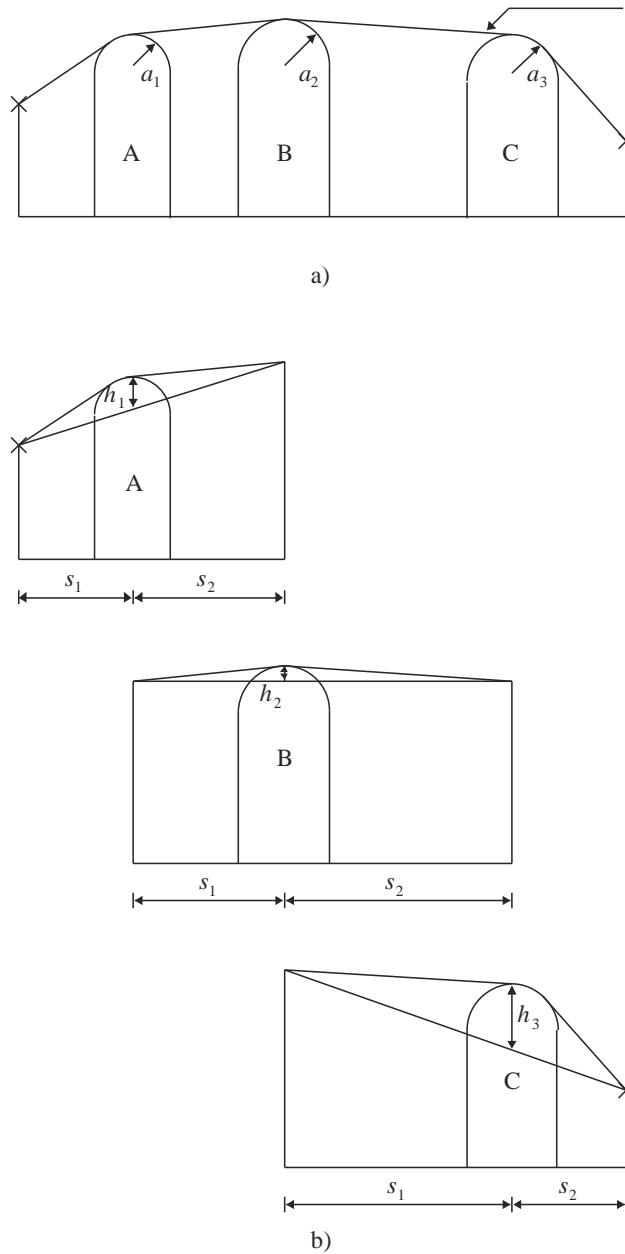
$$k: \text{ effective Earth-radius factor.}$$

A test is now applied to determine whether any group of two or more string points should represent the same terrain obstruction. For samples at spacings of 250 m or less any group of string points which are consecutive profile samples, other than the transmitter or receiver, should be treated as one obstruction.

Each obstruction is now modelled as a cylinder, as illustrated in Fig. 13. The geometry of each individual cylinder corresponds with Fig. 8c). Note that in Fig. 13 the distances  $s_1, s_2$  for each cylinder are shown as measured horizontally between the vertex points, and that for near-horizontal rays these distances approximate to the slope distances  $d_1$  and  $d_2$  in Fig. 8c). For ray angles to the horizontal greater than about  $5^\circ$  it may be necessary to set  $s_1$  and  $s_2$  to the inter-vertex slope distances  $d_1$  and  $d_2$ .

FIGURE 13

The cascaded cylinder model a), overall problem b), details



P.0526-13

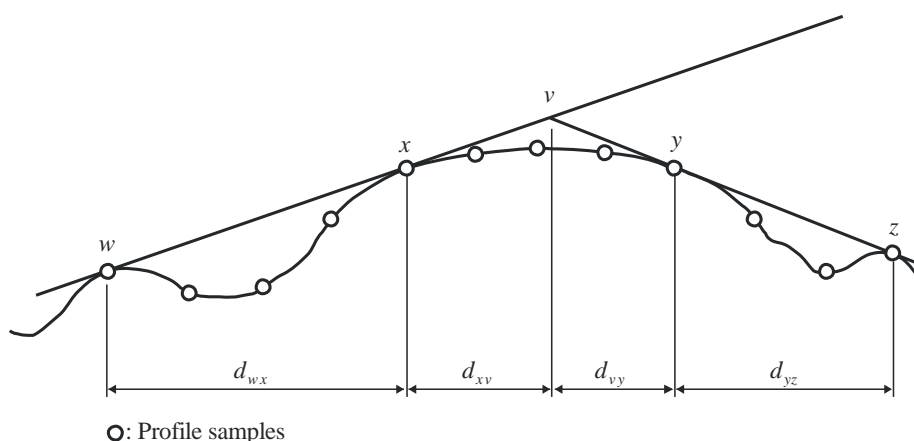
Similarly in Fig. 13, the height  $h$  of each cylinder is shown as measured vertically from its vertex down to the straight line joining the adjacent vertex or terminal points. The value of  $h$  for each cylinder corresponds to  $h$  in Fig. 8c). Again, for near-horizontal rays the cylinder heights may be computed as though vertical, but for steeper ray angles it may be necessary to compute  $h$  at right angles to the baseline of its cylinder.

Figure 14 illustrates the geometry for an obstruction consisting of more than one string point. The following points are indicated by:

- w: closest string point or terminal on the transmitter side of the obstruction which is not part of the obstruction
- x: string point forming part of the obstruction which is closest to the transmitter
- y: string point forming part of the obstruction which is closest to the receiver

- z: closest string point or terminal on the receiver side of the obstruction which is not part of the obstruction
- v: vertex point made by the intersection of incident rays above the obstruction.

FIGURE 14  
Geometry of a multipoint obstacle



P.0526-14

The letters  $w$ ,  $x$ ,  $y$  and  $z$  will also be indices to the arrays of profile distance and height samples. For an obstruction consisting of an isolated string point,  $x$  and  $y$  will have the same value, and will refer to a profile point which coincides with the vertex. Note that for cascaded cylinders, points  $y$  and  $z$  for one cylinder are points  $w$  and  $x$  for the next, etc.

A step-by-step method for fitting cylinders to a general terrain profile is described in Attachment 1 to Annex 1. Each obstruction is characterized by  $w$ ,  $x$ ,  $y$  and  $z$ . The method of Attachment 1 to Annex 1 is then used to obtain the cylinder parameters  $s_1$ ,  $s_2$ ,  $h$  and  $R$ . Having modelled the profile in this way, the diffraction loss for the path is computed as the sum of three terms:

- the sum of diffraction losses over the cylinders;
- the sum of sub-path diffraction between cylinders (and between cylinders and adjacent terminals);
- a correction term.

The total diffraction loss, in dB relative to free-space loss, may be written:

$$L_d = \sum_{i=1}^N L'_i + L''(w x)_1 + \sum_{i=1}^N L''(y z)_i - 20 \log C_N \quad \text{dB} \quad (45)$$

where:

- $L'_i$ : diffraction loss over the  $i$ -th cylinder calculated by the method of § 4.2
- $L''(w x)_1$ : sub-path diffraction loss for the section of the path between points  $w$  and  $x$  for the first cylinder
- $L''(y z)_i$ : sub-path diffraction loss for the section of the path between points  $y$  and  $z$  for all cylinders
- $C_N$ : correction factor to account for spreading loss due to diffraction over successive cylinders.

Attachment 2 to Annex 1 gives a method for calculating  $L''$  for each LoS section of the path between obstructions.

The correction factor,  $C_N$ , is calculated using:

$$C_N = (P_a / P_b)^{0.5} \quad (46)$$

where:

$$P_a = s_1 \prod_{i=1}^N [(s_2)_i] \left( s_1 + \sum_{j=1}^N [(s_2)_j] \right) \quad (47)$$

$$P_b = (s_1)_1 (s_2)_N \prod_{i=1}^N [(s_1)_i + (s_2)_i] \quad (48)$$

and the suffices to round brackets indicate individual cylinders.

#### 4.5 Method for a general terrestrial path

This method is recommended for situations where an automatic process is required to predict diffraction loss for any type of path as defined by a profile, whether LoS or trans-horizon, and whether the terrain is rough or smooth. This model is based on the Bullington construction, but also makes use of the spherical Earth diffraction model as described in § 3.2. These models are combined so that for a completely smooth path, the result will be the same as the spherical Earth model.

The path must be described by a profile consisting of samples of terrain height in metres above sea level for a succession of distances from one terminal to the other. Unlike the profile required in § 4.4, the first and last points of this profile,  $(d_1, h_1)$  and  $(d_n, h_n)$ , must give terrain height underneath the two antennas, and the antenna heights above ground must be supplied separately.

In this model, there is no requirement for the profile points to be equally spaced. However, it is important that the maximum point spacing is not large compared to the sample spacing of the topographic data from which it is extracted. It is particularly inadvisable to represent a section of constant height profile, such as water, by a first and last point separated by the length of the flat section of the path. The model performs no interpolation between profile points, and due to Earth curvature a large distance between profile points, however flat the profile between, can lead to significant errors.

Where urbanization or tree cover exists along the profile, it will normally improve accuracy to add a representative clutter height to bare earth terrain heights. This should not be done for the terminal locations (first and last profile points) and care is needed close to the terminals to ensure that the addition of cover heights does not cause an unrealistic increase in the horizon elevation angles as seen by each antenna. If a terminal is in an area with ground cover and below the representative cover height, it may be preferable to raise the terminal to the cover height for the application of this model, and to use a separate height-gain correction for the additional loss actually experienced by the terminal in its actual (lower) position.

This method should be used when there is no *a priori* information as to the nature of the propagation path or of possible terrain obstructions. This is typical of the case where a computer program is used for profiles selected from a terrain height database on a fully automatic basis, with no individual inspection of path characteristics. The method gives reliable results for all types of path, LoS or trans-horizon, rough or smooth, or over the sea or large bodies of water.

The method contains two sub-models:

- a) the Bullington diffraction method used with a tapered correction to provide a smooth transition between LoS and trans-horizon;

b) the spherical Earth method given in § 3.2.

The Bullington part of the method is used twice. The following subsection gives a general description of the Bullington calculation.

#### 4.5.1 Bullington model

In the following equations slopes are calculated in m/km relative to the baseline joining sea level at the transmitter to sea level at the receiver. The distance and height of the  $i$ -th profile point are  $d_i$  km and  $h_i$  m above sea level respectively,  $i$  takes values from 1 to  $n$  where  $n$  is the number of profile points, and the complete path length is  $d$  km. For convenience the terminals at the start and end of the profile are referred to as transmitter and receiver, with heights in m above sea level  $h_{ts}$  and  $h_{rs}$ , respectively. Effective Earth curvature  $C_e$  km<sup>-1</sup> is given by  $1/r_e$  where  $r_e$  is effective Earth radius in km. Wavelength in metres is represented by  $\lambda$ .

Find the intermediate profile point with the highest slope of the line from the transmitter to the point.

$$S_{tim} = \max \left[ \frac{h_i + 500C_e d_i (d - d_i) - h_{ts}}{d_i} \right] \quad \text{m/km} \quad (49)$$

where the profile index  $i$  takes values from 2 to  $n - 1$ .

Calculate the slope of the line from transmitter to receiver assuming an LoS path:

$$S_{tr} = \frac{h_{rs} - h_{ts}}{d} \quad \text{m/km} \quad (50)$$

Two cases must now be considered.

*Case 1. Path is LoS*

If  $S_{tim} < S_{tr}$  the path is LoS.

Find the intermediate profile point with the highest diffraction parameter  $v$ :

$$v_{\max} = \max \left\{ \left[ h_i + 500C_e d_i (d - d_i) - \frac{h_{ts}(d - d_i) + h_{rs}d_i}{d} \right] \sqrt{\frac{0.002d}{\lambda d_i (d - d_i)}} \right\} \quad (51)$$

where the profile index  $i$  takes values from 2 to  $n - 1$ .

In this case, the knife-edge loss for the Bullington point is given by:

$$L_{uc} = J(v_{\max}) \quad \text{dB} \quad (52)$$

where the function  $J$  is given by equation (31) for  $v_b$  greater than  $-0.78$ , and is zero otherwise.

*Case 2. Path is trans-horizon*

If  $S_{tim} \geq S_{tr}$  the path is trans-horizon.

Find the intermediate profile point with the highest slope of the line from the receiver to the point.

$$S_{rim} = \max \left[ \frac{h_i + 500C_e d_i (d - d_i) - h_{rs}}{d - d_i} \right] \quad \text{m/km} \quad (53)$$

where the profile index  $i$  takes values from 2 to  $n - 1$ .

Calculate the distance of the Bullington point from the transmitter:

$$d_b = \frac{h_{rs} - h_{ts} + S_{rim}d}{S_{im} + S_{rim}} \quad \text{km} \quad (54)$$

Calculate the diffraction parameter,  $v_b$ , for the Bullington point:

$$v_b = \left[ h_{ts} + S_{tim} d_b - \frac{h_{ts}(d-d_b) + h_{rs}d_b}{d} \right] \sqrt{\frac{0.002d}{\lambda d_b (d-d_b)}} \quad (55)$$

In this case, the knife-edge loss for the Bullington point is given by:

$$L_{uc} = J(v_b) \quad \text{dB} \quad (56)$$

For  $L_{uc}$  calculated using either equation (52) or (56), Bullington diffraction loss for the path is now given by:

$$L_b = L_{uc} + [1 - \exp(-L_{uc}/6)](10 + 0.02 d) \quad (57)$$

#### 4.5.2 Complete method

Use the method in § 4.5.1 for the actual terrain profile and antenna heights. Set the resulting Bullington diffraction loss for the actual path,  $L_{ba}$  dB, to  $L_b$  as given by equation (57).

Find the effective transmitter and receiver heights relative to a smooth surface fitted to the profile.

Calculate initial provisional values for the heights of the smooth surface at the transmitter and receiver ends of the path, as follows:

$$v_1 = \sum_{i=2}^n (d_i - d_{i-1})(h_i + h_{i-1}) \quad (58)$$

$$v_2 = \sum_{i=2}^n (d_i - d_{i-1}) [h_i (2d_i + d_{i-1}) + h_{i-1} (d_i + 2d_{i-1})] \quad (59)$$

$$h_{stip} = \left( \frac{2v_1 d - v_2}{d^2} \right) \quad (60a)$$

$$h_{srip} = \left( \frac{v_2 - v_1 d}{d^2} \right) \quad (60b)$$

Find the highest obstruction height above the straight-line path from transmitter to receiver  $h_{obs}$ , and the horizon elevation angles  $\alpha_{obt}$ ,  $\alpha_{obr}$ , all based on flat-Earth geometry, according to:

$$h_{obs} = \max \{h_{obi}\} \quad \text{m} \quad (61a)$$

$$\alpha_{obt} = \max \{h_{obi}/d_i\} \quad \text{mrad} \quad (61b)$$

$$\alpha_{obr} = \max \{h_{obi}/(d-d_i)\} \quad \text{mrad} \quad (61c)$$

where:

$$h_{obi} = h_i - [h_{ts}(d-d_i) + h_{rs}d_i]/d \quad \text{m} \quad (61d)$$

and the profile index  $i$  takes values from 2 to  $(n-1)$ .

Calculate provisional values for the heights of the smooth surface at the transmitter and receiver ends of the path:

If  $h_{obs}$  is less than or equal to zero, then:

$$h_{stp} = h_{stip} \quad \text{masl} \quad (62a)$$

$$h_{srp} = h_{srip} \quad \text{masl} \quad (62b)$$

otherwise:

$$h_{stp} = h_{stip} - h_{obs}g_t \quad \text{masl} \quad (62c)$$

$$h_{srp} = h_{srip} - h_{obs}g_r \quad \text{masl} \quad (62d)$$

where:

$$g_t = \alpha_{obt} / (\alpha_{obt} + \alpha_{obr}) \quad (62e)$$

$$g_r = \alpha_{obr} / (\alpha_{obt} + \alpha_{obr}) \quad (62f)$$

Calculate final values for the heights of the smooth surface at the transmitter and receiver ends of the path:

If  $h_{stp}$  is greater than  $h_1$  then:

$$h_{st} = h_1 \quad \text{masl} \quad (63a)$$

otherwise:

$$h_{st} = h_{stp} \quad \text{masl} \quad (63b)$$

If  $h_{srp}$  is greater than  $h_n$  then:

$$h_{sr} = h_n \quad \text{masl} \quad (63c)$$

otherwise:

$$h_{sr} = h_{srp} \quad \text{masl} \quad (63d)$$

Use the method in § 4.5.1 for a smooth profile by setting all profile heights  $h_i$  to zero, and with modified antenna heights:

$$h'_{ts} = h_{ts} - h_{st} \quad \text{masl} \quad (64a)$$

$$h'_{rs} = h_{rs} - h_{sr} \quad \text{masl} \quad (64b)$$

Set the resulting Bullington diffraction loss for the smooth path,  $L_{bs}$  dB, to  $L_b$  as given by equation (57).

Use the method for diffraction over spherical earth given in § 3.2 for the actual path length  $d$  km and with:

$$h_1 = h'_{ts} \quad \text{m} \quad (65a)$$

$$h_2 = h'_{rs} \quad \text{m} \quad (65b)$$

Set the resulting spherical-earth diffraction loss,  $L_{sph}$  dB, to  $A$  as given by equation (25).

The diffraction loss for the general path is now given by:

$$L = L_{ba} + \max\{L_{sph} - L_{bs}, 0\} \quad \text{dB} \quad (66)$$

## 5 Diffraction by thin screens

The following methods assume that the obstruction is in the form of a thin screen. They can be applied to propagation around an obstacle or through an aperture.

### 5.1 Finite-width screen

Interference suppression for a receiving site (e.g. a small earth station) may be obtained by an artificial screen of finite width transverse to the direction of propagation. For this case the field in the shadow of the screen may be calculated by considering three knife-edges, i.e. the top and the two sides of the screen. Constructive and destructive interference of the three independent contributions will result in rapid fluctuations of the field strength over distances of the order of a wavelength. The following simplified model provides estimates for the average and minimum diffraction loss as a function of location. It consists of adding the amplitudes of the individual contributions for an estimate of the minimum diffraction loss and a power addition to obtain an estimate of the average diffraction loss. The model has been tested against accurate calculations using the uniform theory of diffraction (UTD) and high-precision measurements.

*Step 1:* Calculate the geometrical parameter  $v$  for each of the three knife-edges (top, left side and right side) using any of equations (26) to (29).

*Step 2:* Calculate the loss factor  $j(v) = 10^{J(v)/20}$  associated with each edge from equation (31).

*Step 3:* Calculate minimum diffraction loss  $J_{min}$  from:

$$J_{min}(v) = -20 \log \left[ \frac{1}{j_1(v)} + \frac{1}{j_2(v)} + \frac{1}{j_3(v)} \right] \quad \text{dB} \quad (67)$$

or, alternatively,

*Step 4:* Calculate average diffraction loss  $J_{av}$  from:

$$J_{av}(v) = -10 \log \left[ \frac{1}{j_1^2(v)} + \frac{1}{j_2^2(v)} + \frac{1}{j_3^2(v)} \right] \quad \text{dB} \quad (68)$$

### 5.2 Diffraction by rectangular apertures and composite apertures or screens

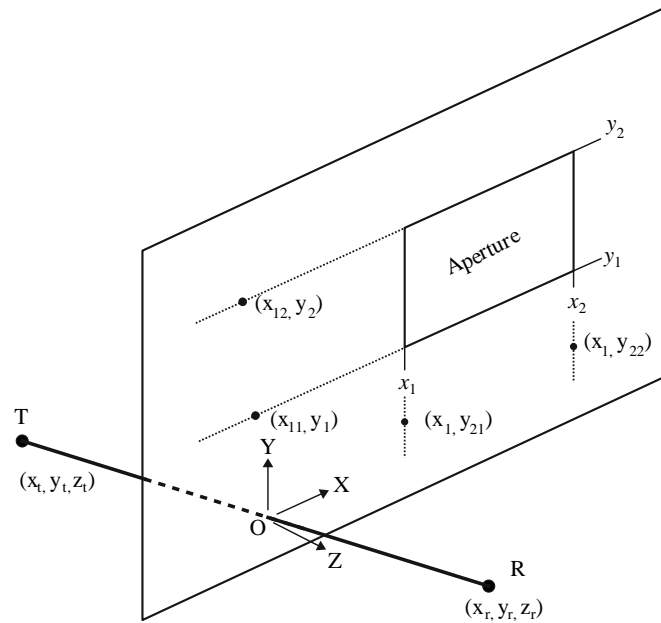
The method described below can be used to predict the diffraction loss due to a rectangular aperture in an otherwise totally absorbing thin screen. The method can be extended to cover several rectangular apertures or finite screens, and is thus an alternative method for the finite-width screen discussed in § 5.1.

#### 5.2.1 Diffraction by a single rectangular aperture

Figure 15 shows the geometry used to represent a rectangular aperture in an infinite totally absorbing thin screen.



FIGURE 15  
Geometry for a single rectangular aperture



The positions of the aperture edges,  $x_1$ ,  $x_2$ ,  $y_1$  and  $y_2$ , are given in a Cartesian coordinate system with origin at the point where the straight line from transmitter T at coordinates  $x_t$ ,  $y_t$ ,  $z_t$ , to receiver R at coordinates  $x_r$ ,  $y_r$ ,  $z_r$ , passes through the screen in the X-Y plane, with propagation not necessarily parallel to the Z axis. The origin is on the plane of the screen.

The angle  $\theta_p$  between the direction of propagation and the Z axis is

$$\theta_p = \arctan \left( \frac{\sqrt{(x_r - x_t)^2 + (y_r - y_t)^2}}{z_r - z_t} \right) \quad \text{rad} \quad (69)$$

The field strength,  $e_a$ , at the receiver in linear units normalized to free space, and in complex form, may be evaluated accurately for small  $\theta_p$  by the Fresnel integral method of § 5.2.1.1, or with reasonable accuracy for any  $\theta_p$  by the semi-empirical method of § 5.2.1.2.

The corresponding diffraction loss  $L_a$  is given by:

$$L_a = -20 \log (|e_a|) \quad \text{dB} \quad (70)$$

### 5.2.1.1 Fresnel integral method

$$e_a(x_1, x_2, y_1, y_2) = 0.5(C_x S_y + S_x C_y) + j 0.5(S_x S_y - C_x C_y) \quad (71)$$

where:

$$C_x = C(v_{x2}) - C(v_{x1}) \quad (72a)$$

$$C_y = C(v_{y2}) - C(v_{y1}) \quad (72b)$$

$$S_x = S(v_{x2}) - S(v_{x1}) \quad (72c)$$

$$S_y = S(v_{y2}) - S(v_{y1}) \quad (72d)$$

$C(v)$  and  $S(v)$  are as given in equations (7a) and (7b) and may be evaluated from the complex Fresnel coefficient using equations (8a) and (8b).

The four diffraction parameters  $v_{x1}$ ,  $v_{x2}$ ,  $v_{y1}$ , and  $v_{y2}$  are:

$$v_{x1} = \text{sgn}(x_1) \sqrt{\frac{2}{\lambda} |x_1|^{1.18} \left( \frac{1}{z_r} - \frac{1}{z_t} \right)^{0.18} |\phi_{21}|^{0.82}} \quad (73a)$$

$$v_{x2} = \text{sgn}(x_2) \sqrt{\frac{2}{\lambda} |x_2|^{1.18} \left( \frac{1}{z_r} - \frac{1}{z_t} \right)^{0.18} |\phi_{22}|^{0.82}} \quad (73b)$$

$$v_{y1} = \text{sgn}(y_1) \sqrt{\frac{2}{\lambda} |y_1|^{1.18} \left( \frac{1}{z_r} - \frac{1}{z_t} \right)^{0.18} |\phi_{11}|^{0.82}} \quad (73c)$$

$$v_{y2} = \text{sgn}(y_2) \sqrt{\frac{2}{\lambda} |y_2|^{1.18} \left( \frac{1}{z_r} - \frac{1}{z_t} \right)^{0.18} |\phi_{12}|^{0.82}} \quad (73d)$$

with:

$$\phi_{21} = \arctan\left(\frac{x_1 - x_r}{z_r}\right) - \arctan\left(\frac{x_1 - x_t}{z_t}\right) \quad \text{rad} \quad (73e)$$

$$\phi_{22} = \arctan\left(\frac{x_2 - x_r}{z_r}\right) - \arctan\left(\frac{x_2 - x_t}{z_t}\right) \quad \text{rad} \quad (73f)$$

$$\phi_{11} = \arctan\left(\frac{y_1 - y_r}{z_r}\right) - \arctan\left(\frac{y_1 - y_t}{z_t}\right) \quad \text{rad} \quad (73g)$$

$$\phi_{12} = \arctan\left(\frac{y_2 - y_r}{z_r}\right) - \arctan\left(\frac{y_2 - y_t}{z_t}\right) \quad \text{rad} \quad (73h)$$

### 5.2.1.2 Semi-empirical method

For reasonable accuracy at any  $\theta_p$ , the following method does not require the Fresnel integrals  $C(v)$  and  $S(v)$ :

$$e_a = \prod_{i=1}^2 \left[ \text{sgn}(\phi_{i1}) \left( \frac{1}{2} - \frac{ph_{i1}}{Ph} G_{i1} \right) - \text{sgn}(\phi_{i2}) \left( \frac{1}{2} - \frac{ph_{i2}}{Ph} G_{i2} \right) \right] \quad (74)$$

where:

$$G_{ij} = \cos\left(\frac{\phi_{ij}}{2}\right) \left[ \frac{1}{2} - \frac{1}{\pi} \arctan(1.4v_{ij}) \right] \quad (75)$$

with  $\phi_{ij}$  from equations (73e) to (73h), and

$$v_{ij} = 2 \sqrt{\frac{1}{\lambda} (D_{t-proj-ij} + D_{r-proj-ij} - r_{proj-i})} \quad (76)$$

$$r_{proj-1} = \sqrt{(z_r - z_t)^2 + (y_r - y_t)^2} \quad (77a)$$

$$r_{proj-2} = \sqrt{(z_r - z_t)^2 + (x_r - x_t)^2} \quad (77b)$$

$$D_{t-proj-11} = \sqrt{z_t^2 + (y_1 - y_t)^2} \quad (78a)$$

$$D_{t-proj-12} = \sqrt{z_t^2 + (y_2 - y_t)^2} \quad (78b)$$

$$D_{t-proj-21} = \sqrt{z_t^2 + (x_1 - x_t)^2} \quad (78c)$$

$$D_{t-proj-22} = \sqrt{z_t^2 + (x_2 - x_t)^2} \quad (78d)$$

$$D_{r-proj-11} = \sqrt{z_r^2 + (y_1 - y_r)^2} \quad (78e)$$

$$D_{r-proj-12} = \sqrt{z_r^2 + (y_2 - y_r)^2} \quad (78f)$$

$$D_{r-proj-21} = \sqrt{z_r^2 + (x_1 - x_r)^2} \quad (78g)$$

$$D_{r-proj-22} = \sqrt{z_r^2 + (x_2 - x_r)^2} \quad (78h)$$

Evaluate  $D_{11}$ ,  $D_{12}$ ,  $D_{21}$ ,  $D_{22}$ :

$$D_{ij} = \sqrt{(z_r)^2 + (y_r - y_{ij})^2 + (x_r - x_{ij})^2} + \sqrt{(z_t)^2 + (y_t - y_{ij})^2 + (x_t - x_{ij})^2} \quad (79)$$

where, if  $D_{r-proj-1j} \neq D_{t-proj-1j}$

$$x_{1j} = \frac{x_t (D_{r-proj-1j})^2 - x_r (D_{t-proj-1j})^2 - D_{t-proj-1j} D_{r-proj-1j} (x_t - x_r)}{(D_{r-proj-1j})^2 - (D_{t-proj-1j})^2}, \quad (80a)$$

or if  $D_{r-proj-1j} = D_{t-proj-1j}$

$$x_{1j} = \frac{x_t + x_r}{2}, \quad (80b)$$

and if  $D_{r-proj-2j} \neq D_{t-proj-2j}$

$$y_{2j} = \frac{y_t (D_{r-proj-2j})^2 - y_r (D_{t-proj-2j})^2 - D_{t-proj-2j} D_{r-proj-2j} (y_t - y_r)}{(D_{r-proj-2j})^2 - (D_{t-proj-2j})^2}, \quad (81a)$$

or if  $D_{r-proj-2j} = D_{t-proj-2j}$

$$y_{2j} = \frac{y_t + y_r}{2} \quad (81b)$$

and

$$y_{1j} = y_j, x_{2j} = x_j \quad (82)$$

using  $ph_{11}, ph_{12}, ph_{21}, ph_{22}$ , from

$$ph_{ij} = \exp\left(\frac{-j2\pi D_{ij}}{\lambda}\right) \quad (83)$$

and  $Ph$ :

$$Ph = \exp\left(\frac{-j2\pi r}{\lambda}\right) \quad (84)$$

### 5.2.2 Diffraction by composite apertures or screens

The method for a single rectangular aperture can be extended as follows:

Since in the linear units normalized to free space of equations (71) or (74) the free-space field is given by  $1.0 + j 0.0$ , the normalized complex field  $e_s$  due to a single rectangular screen (isolated from ground) is given by:

$$e_s = 1.0 - e_a \quad (85)$$

where  $e_a$  is calculated using equations (71) or (74) for an aperture of the same size and position as the screen.

- The normalized field due to combinations of several rectangular apertures or isolated screens can be calculated by adding the results of equations (71) or (74).
- Arbitrarily shaped apertures or screens can be approximated by suitable combinations of rectangular apertures or screens.
- Since the  $C(v)$  and  $S(v)$  integrals converge to  $0.5 + j 0.5$  as  $v$  approaches infinity, equation (71) can be applied to rectangles of unlimited extent in one or more directions.

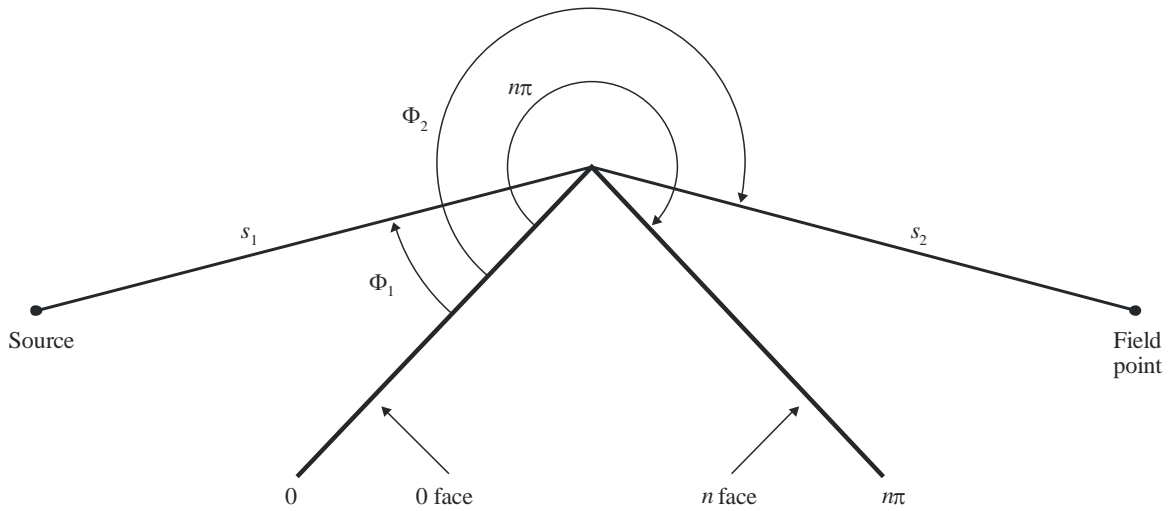
## 6 Diffraction over a finitely conducting wedge

The method described below can be used to predict the diffraction loss due to a finitely conducting wedge. Suitable applications are for diffraction around the corner of a building or over the ridge of a roof, or where terrain can be characterized by a wedge-shaped hill. The method requires the conductivity and relative dielectric constant of the obstructing wedge, and assumes that no transmission occurs through the wedge material.

The method is based on UTD. It takes account of diffraction in both the shadow and line-of-sight region, and a method is provided for a smooth transition between these regions.

The geometry of a finitely conducting wedge-shaped obstacle is illustrated in Fig. 16.

FIGURE 16  
Geometry for application of UTD wedge diffraction



P0526-16

The UTD formulation for the electric field at the field point, specializing to two dimensions, is:

$$e_{UTD} = e_0 \frac{\exp(-jk s_1)}{s_1} D_{\parallel}^{\perp} \cdot \sqrt{\frac{s_1}{s_2(s_1 + s_2)}} \cdot \exp(-jk s_2) \quad (86)$$

where:

- $e_{UTD}$ : electric field at the field point
- $e_0$ : relative source amplitude
- $s_1$ : distance from source point to diffracting edge
- $s_2$ : distance from diffracting edge to field point
- $k$ : wave number  $2\pi/\lambda$
- $D_{\parallel}^{\perp}$ : diffraction coefficient depending on the polarization (parallel or perpendicular to the plane of incidence) of the incident field on the edge

and  $s_1$ ,  $s_2$  and  $\lambda$  are in self-consistent units.

The diffraction coefficient for a finitely conducting wedge is given as:

$$D_{\parallel}^{\perp} = \frac{-\exp(-j\pi/4)}{2n\sqrt{2\pi k}} \left\{ \begin{array}{l} \cot\left(\frac{\pi + (\Phi_2 - \Phi_1)}{2n}\right) \cdot F(kL\alpha^+(\Phi_2 - \Phi_1)) \\ + \cot\left(\frac{\pi - (\Phi_2 - \Phi_1)}{2n}\right) \cdot F(kL\alpha^-(\Phi_2 - \Phi_1)) \\ + R_0^{\perp} \cdot \cot\left(\frac{\pi - (\Phi_2 + \Phi_1)}{2n}\right) \cdot F(kL\alpha^-(\Phi_2 + \Phi_1)) \\ + R_n^{\perp} \cdot \cot\left(\frac{\pi + (\Phi_2 + \Phi_1)}{2n}\right) \cdot F(kL\alpha^+(\Phi_2 + \Phi_1)) \end{array} \right\} \quad (87)$$

where:

- $\Phi_1$ : incidence angle, measured from incidence face (0 face)
- $\Phi_2$ : diffraction angle, measured from incidence face (0 face)

$n$ : external wedge angle as a multiple of  $\pi$  radians (actual angle =  $n\pi$  (rad))

$$j = \sqrt{-1}$$

and where  $F(x)$  is a Fresnel integral:

$$F(x) = 2j\sqrt{x} \cdot \exp(jx) \cdot \int_{\sqrt{x}}^{\infty} \exp(-jt^2) dt \quad (88)$$

$$\int_{\sqrt{x}}^{\infty} \exp(-jt^2) dt = \sqrt{\frac{\pi}{8}}(1 - j) - \int_0^{\sqrt{x}} \exp(-jt^2) dt \quad (89)$$

The integral may be calculated by numerical integration.

Alternatively a useful approximation is given by:

$$\int_{\sqrt{x}}^{\infty} \exp(-jt^2) dt = \sqrt{\frac{\pi}{2}} A(x) \quad (90)$$

where:

$$A(x) = \begin{cases} \frac{1 - j}{2} - \exp(-jx) \sqrt{\frac{x}{4}} \sum_{n=0}^{11} \left[ (a_n + jb_n) \left(\frac{x}{4}\right)^n \right] & \text{if } x < 4 \\ -\exp(-jx) \sqrt{\frac{4}{x}} \sum_{n=0}^{11} \left[ (c_n + jd_n) \left(\frac{4}{x}\right)^n \right] & \text{otherwise} \end{cases} \quad (91)$$

and the coefficients  $a, b, c, d$  are given in § 2.7.

$$L = \frac{s_2 \cdot s_1}{s_2 + s_1} \quad (92)$$

$$a^{\pm}(\beta) = 2 \cos^2 \left( \frac{2n\pi N^{\pm} - \beta}{2} \right) \quad (93)$$

where:

$$\beta = \Phi_2 \pm \Phi_1 \quad (94)$$

In equation (45),  $N^{\pm}$  are the integers which most nearly satisfy the equation.

$$N^{\pm} = \frac{\beta \pm \pi}{2n\pi} \quad (95)$$

$R_0^{\perp}, R_n^{\perp}$  are the reflection coefficients for either perpendicular or parallel polarization given by:

$$R^{\perp} = \frac{\sin(\Phi) - \sqrt{\eta - \cos(\Phi)^2}}{\sin(\Phi) + \sqrt{\eta - \cos(\Phi)^2}} \quad (96)$$

$$R^{\parallel} = \frac{\eta \cdot \sin(\Phi) - \sqrt{\eta - \cos(\Phi)^2}}{\eta \cdot \sin(\Phi) + \sqrt{\eta - \cos(\Phi)^2}} \quad (97)$$

where:

$$\begin{aligned} \Phi &= \Phi_1 \text{ for } R_0 \text{ and } \Phi = (n\pi - \Phi_2) \text{ for } R_n \\ \eta &= \varepsilon_r - j \times 18 \times 10^9 \sigma / f \\ \varepsilon_r &: \text{ relative dielectric constant of the wedge material} \\ \sigma &: \text{ conductivity of the wedge material (S/m)} \\ f &: \text{ frequency (Hz).} \end{aligned}$$

Note that if necessary the two faces of the wedge may have different electrical properties.

At shadow and reflection boundaries one of the cotangent functions in equation (87) becomes singular.

However  $D^{\perp}$  remains finite, and can be readily evaluated. The term containing the singular cotangent function is given for small  $\varepsilon$  as:

$$\cot\left(\frac{\pi \pm \beta}{2n}\right) \cdot F(kLa^{\pm}(\beta)) \cong n \cdot \left[ \sqrt{2\pi kL} \cdot \text{sign}(\varepsilon) - 2kL\varepsilon \cdot \exp(j\pi/4) \right] \cdot \exp(j\pi/4) \quad (98)$$

with  $\varepsilon$  defined by:

$$\varepsilon = \pi + \beta - 2\pi nN^+ \quad \text{for } \beta = \Phi_2 + \Phi_1 \quad (99)$$

$$\varepsilon = \pi - \beta + 2\pi nN^- \quad \text{for } \beta = \Phi_2 - \Phi_1 \quad (100)$$

The resulting diffraction coefficient will be continuous at shadow and reflection boundaries, provided that the same reflection coefficient is used when calculating reflected rays.

The field  $e_{LD}$  due to the diffracted ray, plus the LoS ray for  $(\Phi_2 - \Phi_1) < \pi$ , is given by:

$$e_{LD} = \begin{cases} e_{UTD} + \frac{\exp(-jks)}{s} & \text{for } \Phi_2 < \Phi_1 + \pi \\ e_{UTD} & \text{for } \Phi_2 \geq \Phi_1 + \pi \end{cases} \quad (101)$$

where:

$s$ : straight-line distance between the source and field points.

Note that at  $(\Phi_2 - \Phi_1) = \pi$  the 2<sup>nd</sup> cotangent term in equation (87) will become singular, and that the alternative approximation given by equation (98) must be used.

The field strength at the field point (dB) relative to the field which would exist at the field point in the absence of the wedge-shaped obstruction (i.e. dB relative to free space) is given by setting  $e_0$  to unity in equation (86) and calculating:

$$E_{UTD} = 20 \log \left( \left| \frac{s \cdot e_{UTD}}{\exp(-jks)} \right| \right) \quad (102)$$

where:

$s$ : straight-line distance between the source and field points.

Note that, for  $n = 2$  and zero reflection coefficients, this should give the same results as the knife edge diffraction loss curve shown in Fig. 9.

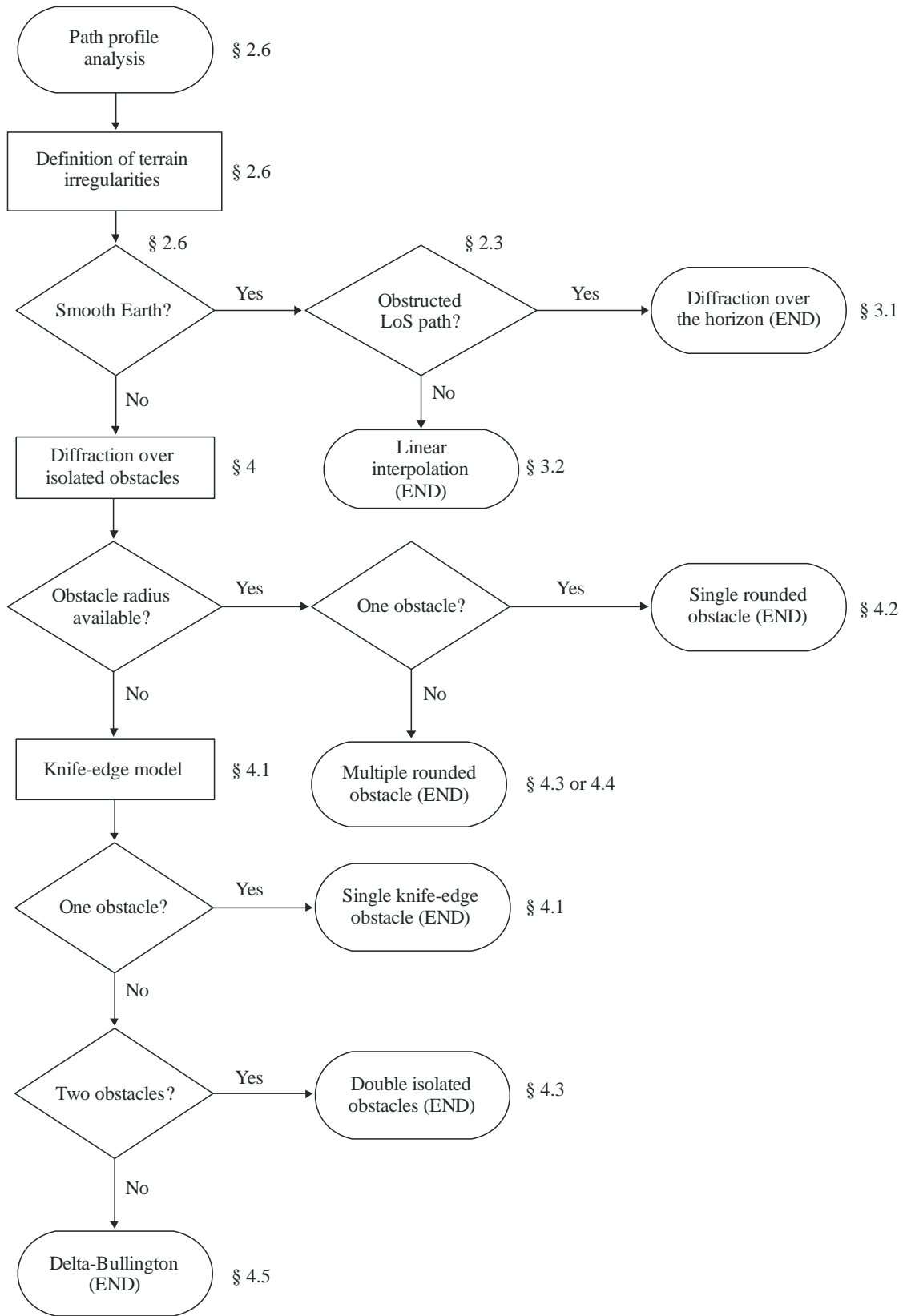
A MathCAD version of the UTD formulation is available from the Radiocommunication Bureau.

**7 Guide to propagation by diffraction**

A general guide for the evaluation of diffraction loss corresponding to §§ 3 and 4 is shown in Fig. 17. This flow chart summarizes the procedure to be adopted in each case.



FIGURE 17  
Guide to propagation by diffraction



## Attachment 1 to Annex 1

### Calculation of cylinder parameters

The following procedure can be used to calculate the cylinder parameters illustrated in Figs 8c) and 14 for each of the terrain obstructions. Self-consistent units are used, and all angles are in radians. The approximations used are valid for radio paths which are within about 5° of horizontal.

#### 1 Diffraction angle and position of vertex

Although not used directly as cylinder parameters, both the diffraction angle over the cylinder and the position of the vertex are required.

The diffraction angle over the obstacle is given by:

$$\theta = \alpha_w + \alpha_z + \alpha_e \quad (103)$$

where  $\alpha_w$  and  $\alpha_z$  are the angular elevations of points  $x$  and  $y$  above the local horizontal as viewed from points  $w$  and  $z$  respectively, given by:

$$\alpha_w = \frac{(h_x - h_w)}{d_{wx}} - \frac{d_{wx}}{2a_e} \quad (104)$$

$$\alpha_z = \frac{(h_y - h_z)}{d_{yz}} - \frac{d_{yz}}{2a_e} \quad (105)$$

and  $\alpha_e$  is the angle subtended by the great-circle distance between points  $w$  and  $z$  given by:

$$\alpha_e = \frac{d_{wz}}{a_e} \quad (106)$$

The distance of the vertex from point  $w$  is calculated according to whether the obstruction is represented by a single profile sample or by more than one.

For a single-point obstruction:

$$d_{wv} = d_{wx} \quad (107)$$

For a multipoint obstruction it is necessary to protect against very small values of diffraction:

$$d_{wv} = \frac{\left[ \left( \alpha_z + \frac{\alpha_e}{2} \right) d_{wz} + h_z - h_w \right]}{\theta} \quad \text{for } \theta \cdot a_e \geq d_{xy} \quad (108a)$$

$$d_{wv} = \frac{(d_{wx} + d_{wy})}{2} \quad \text{for } \theta \cdot a_e < d_{xy} \quad (108b)$$

The distance of point  $z$  from the vertex point is given by:

$$d_{vz} = d_{wz} - d_{wv} \quad (109)$$

The height of the vertex point above sea level is calculated according to whether the obstruction is represented by a single profile sample or by more than one.

For a single point obstruction:

$$h_v = h_x \quad (110)$$

For a multipoint obstruction:

$$h_v = d_{wv} \alpha_w + h_w + \frac{d_{wv}^2}{2a_e} \quad (111)$$

## 2 Cylinder parameters

The cylinder parameters illustrated in Fig. 8c) can now be calculated for each of the terrain obstacles defined by the string analysis:

$d_1$  and  $d_2$  are the positive inter-vertex distances to the obstacles (or terminals) on the transmitter and receiver sides of the obstacle respectively,

and:

$$h = h_v + \frac{d_{wv} d_{vz}}{2a_e} - \frac{(h_w d_{vz} + h_z d_{wv})}{d_{wz}} \quad (112)$$

To calculate the cylinder radius use is made of two further profile samples:

$p$ : the point adjacent to  $x$  on the transmitter side,

and:

$q$ : the point adjacent to  $y$  on the receiver side.

Thus the profile indices  $p$  and  $q$  are given by:

$$p = x - 1 \quad (113)$$

and:

$$q = y + 1 \quad (114)$$

If a point given by  $p$  or  $q$  is a terminal, then the corresponding value of  $h$  should be the terrain height at that point, not the height above sea level of the antenna.

The cylinder radius is calculated as the difference in slope between the profile section  $p-x$  and  $y-q$ , allowing for Earth curvature, divided by the distance between  $p$  and  $q$ .

The distances between profile samples needed for this calculation are:

$$d_{px} = d_x - d_p \quad (115)$$

$$d_{yq} = d_q - d_y \quad (116)$$

$$d_{pq} = d_q - d_p \quad (117)$$

The difference in slope between the  $p-x$  and  $y-q$  profile sections is given in radians by:

$$t = \frac{(h_x - h_p)}{d_{px}} + \frac{(h_y - h_q)}{d_{yq}} - \frac{d_{pq}}{a_e} \quad (118)$$

where  $a_e$  is the effective Earth radius.

The cylinder radius is now given by:

$$R = \left[ d_{pq} / t \right] \left[ 1 - \exp(-4v) \right]^3 \quad (119)$$

where  $v$  is the dimensionless knife-edge parameter in equation (32).

In equation (119), the second factor is an empirical smoothing function applied to the cylinder radius to avoid discontinuities for marginally LoS obstructions.

## Attachment 2 to Annex 1

### Sub-path diffraction losses

#### 1 Introduction

This Attachment provides a method for computing the sub-path diffraction loss for a LoS subsection of a diffraction path. The path has been modelled by cascaded cylinders each characterized by profile points  $w$ ,  $x$ ,  $y$  and  $z$  as illustrated in Figs 13 and 14. The sub-path diffraction is to be calculated for each subsection of the overall path between points represented by  $w$  and  $x$ , or by  $y$  and  $z$ . These are the LoS sections of the path between obstructions, or between a terminal and an obstruction.

The method can also be used for a LoS with sub-path diffraction, in which case it is applied to the entire path.

#### 2 Method

For a LoS section of the profile between profile samples indexed by  $u$  and  $v$ , the first task is to identify the profile sample between but excluding  $u$  and  $v$  which obstructs the largest fraction of the first Fresnel zone for a ray travelling from  $u$  to  $v$ .

To avoid selecting a point which is essentially part of one of the terrain obstacles already modelled as a cylinder, the profile between  $u$  and  $v$  is restricted to a section between two additional indices  $p$  and  $q$ , which are set as follows:

- Set  $p = u + 1$ .
- If both  $p < v$  and  $h_p > h_{p+1}$ , then increase  $p$  by 1 and repeat.
- Set  $q = v - 1$ .
- If both  $q > u$  and  $h_q > h_{q-1}$ , then decrease  $q$  by 1 and repeat.

If  $p = q$  then the sub-path obstruction loss is set to 0. Otherwise the calculation proceeds as follows.

It is now necessary to find the minimum value of normalized clearance,  $C_F$ , given by  $h_z/F_1$ , where in self-consistent units:

$h_z$ : height of ray above profile point

$F_1$ : radius of first Fresnel zone.

The minimum normalized clearance may be written:

$$C_F = \min_{i=p}^q [(h_z)_i / (F_1)_i] \quad (120)$$

where:

$$(h_z)_i = (h_r)_i - (h_t)_i \quad (121)$$

$$(F_1)_i = \sqrt{\lambda \cdot d_{ui} \cdot d_{iv} / d_{uv}} \quad (122)$$

$(h_r)_i$ , the height of the ray above a straight line joining sea level at  $u$  and  $v$  at the  $i$ -th profile point is given by:

$$(h_r)_i = (h_u \cdot d_{iv} + h_v \cdot d_{ui}) / d_{uv} \quad (123)$$

$(h_t)_i$ , the height of the terrain above a straight line joining sea level at  $u$  and  $v$  at the  $i$ -th profile point is given by:

$$(h_t)_i = h_i + d_{ui} \cdot d_{iv} / 2a_e \quad (124)$$

The minimum value of normalized clearance is used to compute the knife-edge diffraction geometrical parameter for the most significant sub-path obstruction:

$$v = -C_F \cdot \sqrt{2} \quad (125)$$

The sub-path diffraction loss  $L''$  is now obtained from equation (31) or Fig. 9.

For some applications it may be undesirable to include sub-path diffraction enhancements. In this case a value of  $L''$  should be set to zero when it would otherwise be negative.

---